Post-buckling optimisation strategy of imperfection sensitive composite shells using Koiter method and Monte Carlo simulation

Francesco S. Liguori[a,*], Antonio Madeo[a], Domenico Magisano[a], Leonardo Leonetti[a], Giovanni Garcea[a]

[a]*Dipartimento di Ingegneria Informatica, Modellistica, Elettronica e Sistemistica Università della Calabria 87036 Rende (Cosenza), Italy*

Abstract

A numerical stochastic strategy for optimising composite elastic shells undergoing buckling is presented. Its scope is to search for the best stacking sequence that maximises the collapse load considering the post-buckling behaviour. Its feasibility is due to a reduced order model built for each material setup starting from a hybrid solid-shell finite element model exploiting a multimodal Koiter method. The approach has no limitations concerning geometry, boundary conditions and material properties distribution. The collapse load is evaluated using a Monte Carlo simulation able to detect the worst imperfection shape, including a-posteriori the imperfections in the reduced order model. For a limited number of parameters the proposal allows to analyse all the possible layups. In the general case, it uses a Monte Carlo scanning of the design parameters with different levels of adaptability. The optimisation of curved panels, also with stiffeners, confirms the feasibility and reliability of the proposed strategy.

Keywords: Composite shells, Post-buckling optimisation, Imperfection sensitivity, Finite element analysis

1. Introduction

Thin-walled composite panels are common in a wide range of engineering applications nowadays, particularly in the aeronautic and aerospace context, where they are often employed as primary structural components. Due to the high strength/weight ratio, the structural response is dominated by buckling and it turns out to be mainly influenced by two factors: the geometry and the elastic properties. While the former is often imposed by the structural functionality and only little changes are possible, the spatial distribution of the material properties, e.g fibre orientations, can be easily tailored in composite shells. As a consequence, an efficient optimisation process of the material is required to obtain the desired structural response, usually defined in terms of deflections and load-carrying capacity. Many manufacturing options are currently available for this purpose: multi-layered and variable thickness composites [1], variable angle tows (VATs) [2] and grid stiffeners [3].

Many optimisation strategies proposed in the literature use the linearised buckling load as the objective function of the design [4–8]. However, in this case, structures may suffer from a phenomenon known as buckling mode interaction, which leads to an unstable post-critical behaviour [9] and a high sensitivity to imperfections, that is a deterioration of their load-bearing capacity due to geometrical, load and material deviations [10]. For this reason, a more reliable design, which takes account of the full geometrically nonlinear behaviour, has also been investigated over the years. In this framework, a collapse state is declared when the applied load exceeds the limit load, for the unstable cases, or because it produces deformations which compromise the usability, accounting for the stiffness reduction that typically characterises the post-buckling

*Corresponding author

Email addresses: francesco.liguori@unical.it (Francesco S. Liguori), antonio.madeo81@unical.it (Antonio Madeo), domenico.magisano@unical.it (Domenico Magisano), leonardo.leonetti@unical.it (Leonardo Leonetti), giovanni.garcea@unical.it (Giovanni Garcea)

regime. Optimising the post-buckling behaviour in terms of collapse load is, however, a challenging task. In fact, a suitable mechanical model and its discrete approximation are required to describe the geometry, the boundary conditions and the structural behaviour accurately. This means that the structural response is generally described by a high number of discrete nonlinear equations, whose solution furnishes the equilibrium path.

The Riks arc-length strategy [11, 12] is the standard tool for solving the discrete nonlinear equations and reconstructing the equilibrium path. Although this approach is effective for assigned data, it is not suitable for an optimisation process, which requires the evaluation of the equilibrium path for each change in the design variables, and for an imperfection sensitivity analysis because the single run is too time consuming with current CPUs. Promising generalisations of the path-following strategy have been presented [13–15] with the aim of performing parametrical studies in a more efficient way.

When addressing the post-buckling optimisation, however, many researchers focused their attention on simplified approaches in order to reduce the computational time of the design stage. They follow, often simultaneously, two main strategies: i) reducing the number of discrete variables by using simplifying assumptions on the mechanical model and its discrete approximation; ii) using optimisation strategies based on a quick prediction of the post-critical behaviour by means of simplifying assumptions on the nonlinear response. Different proposals are available in the literature. In [16] the post-buckling behaviour of compressed rectangular plates is studied by a semi-analytical solution and the layer thicknesses are chosen as optimisation variables. In the optimisation strategy in [17], the collapse load is evaluated by a nonlinear finite element (FE) buckling problem. The algorithm is extended in [18, 19] in order to take account of the worst geometrical imperfection case. A study of the effect of the material degradation in the design of curved stiffened panels is presented in [20]. A Rayleigh–Ritz method which allows the effective treatment of simple geometries is employed in [21] to minimise the maximum transverse displacement of stable VAT plates in the post-buckling regime. In [1] the same authors look for a "Buckle Free" solution, that is limiting the axial stiffness reduction after bifurcation. The optimisation of grid-stiffened structures with curved stiffeners is addressed in [3, 22] by using a hybrid model and surrogate models which allow dimple imperfections to be taken into account. An interesting way of analysing slender structures is offered by strategies based on Koiter's theory of elastic stability [23]. They make use of an asymptotic expansion of the equilibrium equations which allows the description of the initial post-critical behaviour in terms of some variables related to the slope and curvature of the bifurcated branches [24]. These quantities can be optimised in order to obtain the desired structural response. A first attempt in using the Koiter method to perform a minimum weight optimisation of stiffened curved panels, discretised by means of the finite strip method, is proposed in [25]. More recently, in [24, 26], formulations based on simplified structural models and a single buckling mode are used to optimise the post-buckling behaviour of composite and VAT structures.

Despite the difficulties found in modelling the structural problem and predicting the nonlinear behaviour, another tricky issue is the solution of the optimisation problem. This is always expressed, indeed, as a nonlinear and non-convex mathematical programming problem, whose solution is generally computationally expensive and extremely difficult because of the possible presence of multiple local minima. It represents, ultimately, the most penalising aspect of the analysis. Among the others, frequently employed solution strategies are the random search methods [8], genetic algorithms [27] and gradient based techniques such as the method of moving asymptotes [28] and sequential linear programming [29].

In this work, we propose an optimisation strategy for composite shells which uses a reduced order model (ROM), obtained by the solid-shell FE implementation of the multimodal Koiter method proposed in [30, 31], for the approximation of the equilibrium path. In this way, the ROM allows to describe complex structural problem with a number of variables drastically reduced to a few modal amplitudes, making it possible to easily evaluate the interactions among buckling modes. Complex material configurations can also be easily analysed as shown in recent applications to VAT panels [32]. In addition, the solid-shell FE allows an accurate modelling of complex geometrical local features like stiffeners. The accuracy of the ROM has been extensively tested in the estimation of the equilibrium path of shell structures [30, 33] obtaining results as accurate as those of path-following analyses in terms of limit load and initial post-buckling behaviour, also in case of nonlinear pre-buckling path thanks to a stress-displacement formulation. The approach is so efficient that the solution of the optimisation problem can be obtained by a stochastic analysis, which can

be collocated in the framework of the random search methods [34]. The goal is to maximise the collapse load by selecting an optimal stacking sequence of the multi-layered structure. This means to optimise the limit load for the unstable cases and the load required to reach a fixed displacement of a control point for the stable ones. The construction of the ROM, to be performed for each layup, is the most expensive part of the analysis but its cost is of the order of a linearised buckling analysis [10, 30, 32, 33]. The most interesting feature of this strategy is that the sensitivity to geometrical imperfections is easily included in the optimisation process. To this purpose, the collapse load is evaluated statistically by means of a Monte Carlo simulation aimed at detecting the worst imperfection shape in terms of buckling modes combination. This requires the evaluation of the equilibrium path for thousands of randomly generated imperfection shapes in order to estimate the lowest collapse load for each layup. This kind of sensitivity analysis, that is generally very expensive, has conversely a negligible computational cost thanks to the possibility offered by the Koiter method of including a-posteriori, in the ROM of the perfect structure, the effects of the imperfections [31]. In this way, once the ROM of the perfect structure is available, the estimation of the equilibrium path for each imperfection only requires the solution of a small sized nonlinear system, usually of less than ten equations, carried out in fractions of second. The approach can be generalised to generic imperfection shapes either by reconstructing the ROM with the modified geometry or by enlarging the space of the ROM with a base of shapes as in [35, 36]. A stochastic strategy is employed to select random layups. It is a simple multistage process which evaluates the optimal solution as follows: i) an initial searching in the domain of all the possible layups is performed and the best solutions are selected; ii) the optimal solution is obtained by searching in the neighbourhood of the best layups selected in i). For a limited number of the optimisation variables, it will also be shown how the efficiency of the Koiter method makes it possible to analyse all the possible layups by means of a uniform scanning. The effectiveness of the proposed strategy is tested on two structural optimisations regarding a curved panel and a stiffened curved panel in compression taking into account the worst imperfection shape. The result of this work is a novel design tool, totally based on stochastic simulations, able to optimise the post-buckling behaviour of imperfection sensitive composite shells by selecting an optimal stacking sequence. The approach is simple, characterised by an affordable computational cost and has no limitation in the description of geometry, material properties distributions and boundary conditions.
The paper is so organised: in Section 2 the Koiter algorithm for a hybrid solid-shell FE is briefly recalled and the Monte Carlo sensitivity analysis for identifying the worst imperfection shape is defined; in Section 3 we present the optimisation strategy for the design of the stacking sequence; in Section 4 two numerical applications of the method are shown and some observations on the structural behaviour are made. Lastly, in Section 5, the conclusions are drawn.

2. Imperfection sensitivity analysis using Koiter method

Slender composite structures are sensitive to imperfections in many cases. This means that for an assigned set of data, the limit load value and the post-critical behaviour cannot be described properly without considering the effects of imperfections. Among all the possible deviations from the initial data those regarding the geometry are the most significant ones, as shown for instance in [37] for unstiffened cylinders. For this reason, this work focuses on these kind of imperfections considered as linear combinations of buckling modes. In this section, an imperfection sensitivity analysis based on the Koiter method [38] is presented for detecting the worst imperfections by means of a Monte Carlo approach. A solid-shell FE [30, 39, 40] is used to make the method efficient and model the geometry, e.g. stiffeners, accurately.

2.1. Koiter method for solid-shell

The equilibrium equations, once the structure is discretized using the FE method, can be written as

$$\mathbf{r}[\lambda, \mathbf{u}] = \mathbf{s}[\mathbf{u}] - \lambda \hat{\mathbf{p}} = \mathbf{0} \tag{1}$$

where $\mathbf{r}$ is the residual vector, $\mathbf{s}$ is the internal force vector, $\hat{\mathbf{p}}$ is the reference load vector, $\mathbf{u}$ are the FE variables and λ is the load factor. Equation (1) defines a curve in the space $\mathbf{u} - \lambda$, that is the equilibrium

path of the structure. This nonlinear system, whose size is defined by the number of FE variables required to approximate the continuum problem, is usually solved by means of standard Riks arc-length strategies [11]. The Koiter method described in [30] represents an effective alternative because, using a ROM, provides an approximated solution of (1) by means of a reduced system of equations. The steps of the Koiter method are briefly recalled. It uses a nonlinear Cauchy continuum based on a Green strain measure and a hybrid (stress-displacement) solid-shell FE model. In this way the strain energy has a cubic polynomial dependence only from the configuration variables. The algorithm starts with the so-called perfect structure analysis, to be performed once and for all for assigned material data, which consists in the construction of a ROM and the corresponding reduced nonlinear equations defining the equilibrium path of the structure with no imperfections. The geometrical imperfections are then included directly in the reduced equations of the perfect structure by simply changing some terms, allowing an efficient sensitivity analysis.

2.1.1. Perfect structure analysis

The construction of the ROM of the perfect structure consists of the following steps.

1. The initial path tangent $\hat{\mathbf{u}}$ is evaluated by solving the linear system
$$\mathbf{K}_0\hat{\mathbf{u}} = \hat{\mathbf{p}} \tag{2a}$$
where $\mathbf{K}_0 \equiv \mathbf{K}[\mathbf{0}]$ is the tangent matrix evaluated at the rest configuration.
2. A restricted number m of linearised buckling modes and loads can be obtained by the following eigenvalue problem
$$\mathbf{K}[\lambda]\dot{\mathbf{v}} \equiv (\mathbf{K}_0 + \lambda\mathbf{K}_1[\hat{\mathbf{u}}])\dot{\mathbf{v}} = \mathbf{0} \tag{2b}$$
where $\mathbf{K}_1[\hat{\mathbf{u}}]$ is the geometric matrix.
3. The $m \times (m+1)/2$ quadratic correctives $\mathbf{w}_{ij}, \hat{\hat{\mathbf{w}}} \in \mathcal{W}$ are obtained, adopting a Lagrangian multiplier approach (see [41]), by the solution of the linear systems ($i = 1 \dots m, j = i \dots m$)
$$\begin{cases} \mathbf{K}_b\mathbf{w}_{ij} + \mathbf{p}_{ij} = \mathbf{0} \\ \mathbf{w}_{ij}^T\mathbf{K}_1[\hat{\mathbf{u}}]\dot{\mathbf{v}}_k = 0, \quad k = 1 \dots m \end{cases} \qquad \begin{cases} \mathbf{K}_b\hat{\hat{\mathbf{w}}} + \mathbf{p}_{00} = \mathbf{0} \\ \hat{\hat{\mathbf{w}}}^T\mathbf{K}_1[\hat{\mathbf{u}}]\hat{\mathbf{u}} = 0. \end{cases} \tag{2c}$$
where $\mathbf{K}_b = \mathbf{K}[\lambda_b]$, λ_b being a representative value of the buckling loads cluster, usually chosen as the first linearised buckling load, and
$$\mathbf{p}_{ij} = \mathbf{K}_1[\dot{\mathbf{v}}_i]\dot{\mathbf{v}}_i, \quad \mathbf{p}_{00} = \mathbf{K}_1[\hat{\mathbf{u}}]\hat{\mathbf{u}}.$$
The solution of Eq.(2c) can be obtained adopting the iterative scheme proposed in [41] which uses the already decomposed matrix $\mathbf{K}_0$.
4. The ROM of the perfect structure then assumes the following form
$$\mathbf{u}_d[\lambda, \xi_i] = \lambda\hat{\mathbf{u}} + \sum_i \xi_i\dot{\mathbf{v}}_i + \frac{1}{2}\sum_{ij}\xi_i\xi_j\ddot{\mathbf{w}}_{ij} + \frac{1}{2}\lambda^2\hat{\hat{\mathbf{w}}} \tag{2d}$$
where ξ_i are the modal amplitudes.
5. The reduced system of equations can now be obtained projecting the equations $\mathbf{r}[\lambda, \mathbf{u}_d] = \mathbf{0}$ in directions $\dot{\mathbf{v}}_i$, $i = 1..m$, and maintaining the terms up to the 3rd order in ξ. It can be written as
$$\begin{aligned} r_k[\lambda, \xi_i] \equiv &\mu_k[\lambda] + (\lambda_k - \lambda)\xi_k - \frac{1}{2}\lambda^2\sum_{i=1}^{m}\xi_i\mathcal{C}_{ik} + \frac{1}{2}\sum_{i,j=1}^{m}\xi_i\xi_j\mathcal{A}_{ijk} \\ &+ \frac{1}{6}\sum_{i,j,h=1}^{m}\xi_i\xi_j\xi_h\mathcal{B}_{ijhk} = 0, \quad k = 1 \cdots m \end{aligned} \tag{2e}$$

where the coefficients $\mathcal{A}_{ijk}$, $\mathcal{C}_{ik}$ and $\mathcal{B}_{ijhk}$ are scalar quantities evaluated as the sum of element contributions and their expression is reported in [30]. Eqs.(2e) are an algebraic nonlinear system of m equations in the $m+1$ variables λ, $\xi_1 \cdots \xi_m$ that, due to the small size of the system, can be efficiently solved using specialized variants of the arc–length scheme.

Once Eq. (2e) is solved, the equilibrium path in terms of FE variables can be recovered substituting λ, $\xi_1 \cdots \xi_m$ in Eq. (2d).

2.1.2. A posteriori account of geometrical imperfections

Geometrical imperfections can easily be included in the analysis. They are expressed by an initial displacement $\tilde{\mathbf{u}}$, assumed to be a linear combination of known shapes $\bar{\mathbf{u}}_i$,

$$\tilde{\mathbf{u}} = \sum_{i=1}^{n} \tilde{\xi}_i \bar{\mathbf{u}}_i. \tag{3}$$

In this work, the imperfection shapes $\bar{\mathbf{u}}_i$ are chosen as the displacement part of the buckling modes.

The method allows to take account of imperfections in the final stage by simply adding some additional imperfection terms $\tilde{\mu}_k$ to Eq.(2e) that becomes

$$r_k + \tilde{\mu}_k = 0. \tag{4}$$

Over the years, two different approaches have been developed. The first one, as used in [38, 41, 42], modifies the ROM by simply adding the imperfection vector $\tilde{\mathbf{u}}$ to the ROM of perfect structure in Eq.(2d)

$$\mathbf{u}_d[\lambda, \xi_i] = \tilde{\mathbf{u}} + \lambda \hat{\mathbf{u}} + \mathbf{v}[\xi_i] + \mathbf{w}[\xi_i, \lambda]. \tag{5}$$

This approach, labelled K_{lin}, proves to be extremely efficient but accurate only for small imperfection amplitudes and almost linear pre-critical behaviour. It is, in any case, a powerful tool to obtain information about the worst imperfection shapes because thousands of imperfections can be analysed in a few seconds.

The second strategy, named K_{quad}, has been recently proposed in [31] and updates the ROM as

$$\mathbf{u}_d[\lambda, \xi_i, \tilde{\xi}_i] = \tilde{\mathbf{u}} + \lambda(\hat{\mathbf{u}} + \tilde{\hat{\mathbf{w}}}) + \sum_i \xi_i(\dot{\mathbf{v}}_i + \dot{\tilde{\mathbf{w}}}_i) + \frac{1}{2}\sum_{ij} \xi_i \xi_j \ddot{\mathbf{w}}_{ij} + \frac{1}{2}\lambda^2 \hat{\hat{\mathbf{w}}}. \tag{6}$$

considering new corrective modes generated by the imperfection, which can be seen as a correction to the initial path tangent and the buckling modes of the perfect structures. They can be evaluated as

$$\begin{cases} \mathbf{K}_b \dot{\tilde{\mathbf{w}}}_{ij} + \tilde{\mathbf{p}}_{ij} & = \mathbf{0} \\ \mathbf{K}_b \hat{\tilde{\mathbf{w}}}_i + \tilde{\mathbf{p}}_{0i} & = \mathbf{0} \end{cases}, \quad \forall \mathbf{w} \in \mathcal{W} \tag{7}$$

where

$$\tilde{\mathbf{p}}_{ij} = \mathbf{K}_1[\bar{\mathbf{v}}_i]\dot{\mathbf{u}}_j, \quad \tilde{\mathbf{p}}_{0i} = \mathbf{K}_1[\hat{\mathbf{u}}]\bar{\mathbf{u}}_i.$$

This approach is a little more expensive than the first one, but is more accurate in the case of nonlinear pre-critical path and increasing imperfection amplitudes. The projection of the FE equations (1) in directions $\dot{\mathbf{v}}_i$, $i = 1..m$ using the updated ROMs furnishes the imperfection effects on the ROM of the perfect structure in terms of the additional coefficients $\tilde{\mu}_k$ in Eq. (4).

The computational cost of the Koiter method with both a-posteriori accounts of the geometrical imperfections is of the order of that required by a standard linearised buckling analysis, that is dominated by the factorization of the matrix $\mathbf{K}_0$.

2.2. A Monte Carlo imperfection sensitivity analysis

The geometrical imperfections are expressed as in Eq.(3) where $\tilde{\xi}_i$ are uniformly random generated numbers that set the maximum imperfection shape to a fixed value

$$\max |\tilde{\mathbf{u}}| = \tilde{u}_{max}. \tag{8}$$

In this way it is possible to obtain a statistical sample of imperfections and to draw, for each of them, the equilibrium path. As is well known, we can have a stable post-critical behaviour, usually characterised by a reduction in the stiffness, or an unstable post-critical path with limit point. The collapse is reached because the applied load exceeds the limit load or because the stiffness reduction leads to deformations which compromise the usability. This means that the collapse load associated to $\tilde{\mathbf{u}}$ can be defined as the minimum between the limit load λ_{lim}, if it exists, and the load $\bar{\lambda}$ related to a fixed displacement of a control point

$$\lambda_c = \min_{\tilde{\mathbf{u}}} \left\{ \lambda_{lim}(\tilde{\mathbf{u}}), \quad \bar{\lambda}(\tilde{\mathbf{u}}) \right\}.$$

Because of the nature of the collapse load, as shown in [43], the frequencies distribution of the limit load is best fitted by a type 1 extreme value distribution, also known as Gumbel max distribution. It defines the probability density function as

$$f(\lambda_c) = \sigma^{-1} \exp\left(\frac{\mu - \lambda_c}{\sigma}\right) \exp\left(-\exp\left(\frac{\mu - \lambda_c}{\sigma}\right)\right) \tag{9}$$

where μ and σ are the location parameter and scale parameter, respectively. It is also useful to define the cumulative distribution function as

$$F(\lambda_c) = \int_{-\infty}^{\lambda_c} f(x)dx \tag{10}$$

which represents the probability that a generic imperfection leads to a collapse load lower than λ_c. By inverting Eq.(10) it is possible to obtain the collapse load $\lambda_{c,x}$ which has the probability of x not being exceeded, that is named as x fractile.

The number of imperfections to include in the sensitivity analysis is based on the convergence of the parameters μ and σ. In particular the number of imperfections starts from an initial value and is increased step by step until the parameters converge. The convergence criterion can be chosen as follows: the variation of μ and σ is limited to a tolerance value ϵ_π between two consecutive steps three times in a row, as expressed, for example for μ, as follows

$$\frac{\mu_j - \mu_i}{\mu_j} \leq \epsilon_\pi \quad \forall i = j-1, \cdots, j-3$$

where j denotes the current step.

3. Optimal layup design

In this section two simple optimisation approaches based on the proposed Koiter method are presented. Even if the proposed approaches are very simple they highlight how thousands of equilibrium path estimates can be effectively performed. More refined stochastic algorithms [34] can also be adopted.

3.1. The optimisation algorithms

This section deals with the optimal design of imperfection sensitive shells. Although we focus on seeking optimum layups for a fixed structural geometry, the procedure is general and can be easily adapted to geometry optimisation. In particular, the optimisation problem consists in searching for the solution which maximizes the collapse load λ_c, as defined in 2.2, that is

$$\begin{aligned} &\underset{\boldsymbol{\vartheta}}{\text{maximize}} \quad \lambda_c(\boldsymbol{\vartheta}) \\ &\text{subject to} \quad \vartheta_i \in \{-90^\circ, -72^\circ, \ldots, 72^\circ, 90^\circ\} \end{aligned}$$

where ϑ_i is the fiber orientation of the ith layer and $\boldsymbol{\vartheta}$ is the vector collecting all ϑ_i. Depending on the way it is searched for in the optimization parameters domain, the procedure can be applied in two ways. The first one, named *Uniform scanning*, is the simplest and can be used when the optimisation involves a few parameters. The second one, called *Random scanning*, is more suitable when the number of parameters increases and it is based on a Monte Carlo like approach.

3.2. Uniform scanning

The approach is based on the simple idea of uniformly scanning the space of the N possible layups. In this way, at the end of the process, the collapse load trend with the parameters is completely known and the actual optimal solution can be easily identified. Even if the number of analyses can be significantly high, the efficiency of the Koiter method makes them possible in a reasonable computational time when the space is defined by a few parameters. It is evident, indeed, that the number of analyses increases exponentially with the dimension of the sought parameter space.

The approach consists of two stages. During the first one the space is uniformly scanned and, for each lamination, an imperfection sensitivity analysis is performed to detect the collapse load. The K_{lin} approach to account a-posteriori for geometrical imperfection, as exposed in 2.1.2, is employed to identify the optimal solutions. The second stage is aimed at checking the best solutions found in stage 1 by repeating the imperfection sensitivity analysis with more restrictive tolerances on the μ and σ parameters, as defined in 2.2, and including their effect using the K_{quad} approach which proves to be more accurate. Finally, the structure with the best layup subjected to the worst imperfection shape is analysed by means of a path-following Riks analysis using the full FE model. The diagram in Fig.1 summarises the steps of the whole process.

3.3. Random scanning

The main problem of uniformly scanning the domain of the optimisation parameters is that the number of analyses can increase enormously and, although the Monte Carlo imperfection sensitivity analysis with the Koiter method is efficient, it can prevent the solution of the problem. The second approach proposed overcomes this problem by also using the Monte Carlo method to detect the best stacking sequence. There are three stages in this process. In the first one, the space of the optimisation parameters is sampled with a fixed number N_1 of uniformly generated random values and for each of them the imperfection sensitivity analysis furnishes the limit load and its fractile. Starting from the best n_1 solutions of stage 1, the second stage better investigates some areas of the domain of interest, that is the areas near to the highest n_1 collapse loads. To this purpose, the Monte Carlo simulation at stage 2 (zooming stage) no longer uses uniform random numbers but a fixed number N_2 of random layups near to the laminations selected at the first stage. The population of layups of interest drastically reduces allowing an efficient estimate of the collapse load even for a large number of parameters. This strategy is particularly suitable for optimising the stacking sequence of imperfection sensitive slender structures because all the layer orientations can be chosen as independent optimisation parameters and their number is usually of the order of tens. In addition, the strategy can be adapted to the specific problem because subsequent zooming stages can be performed to investigate the areas of the domain that seem to be of particular interest from one stage to another until satisfactory results are obtained. After the zooming stage sequences a final stage is performed to validate the n_2 optimal results found in stage 2; it is carried out using the K_{quad} formula to include imperfections effects and with a larger number of imperfection shapes. Lastly, the results are further tested with path following analyses on the selected laminations with the worst imperfection cases. The values of N_1, N_2, n_1 and n_2 can be set for each specific test. Suitable choices are those reported in the numerical results section.

In Fig.2 the approach is summarised. It is written for the particular case of one zooming stage only. The continuum domain of the angles is discretised; its borders are denoted with ϑ_i and ϑ_f, while ϑ_p is the discretisation step. In the subsequent zooming stages the symbol δ is added to the domain borders to define the neighbourhood of the angles it is scanned in.

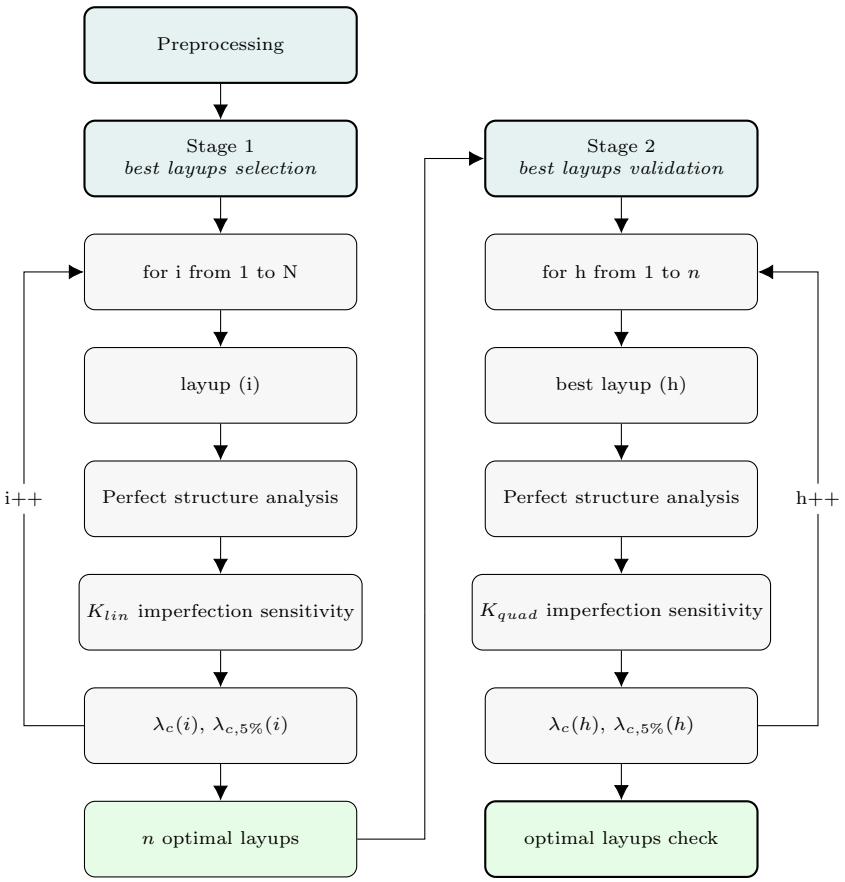

Figure 1: Diagram of the uniform scanning.

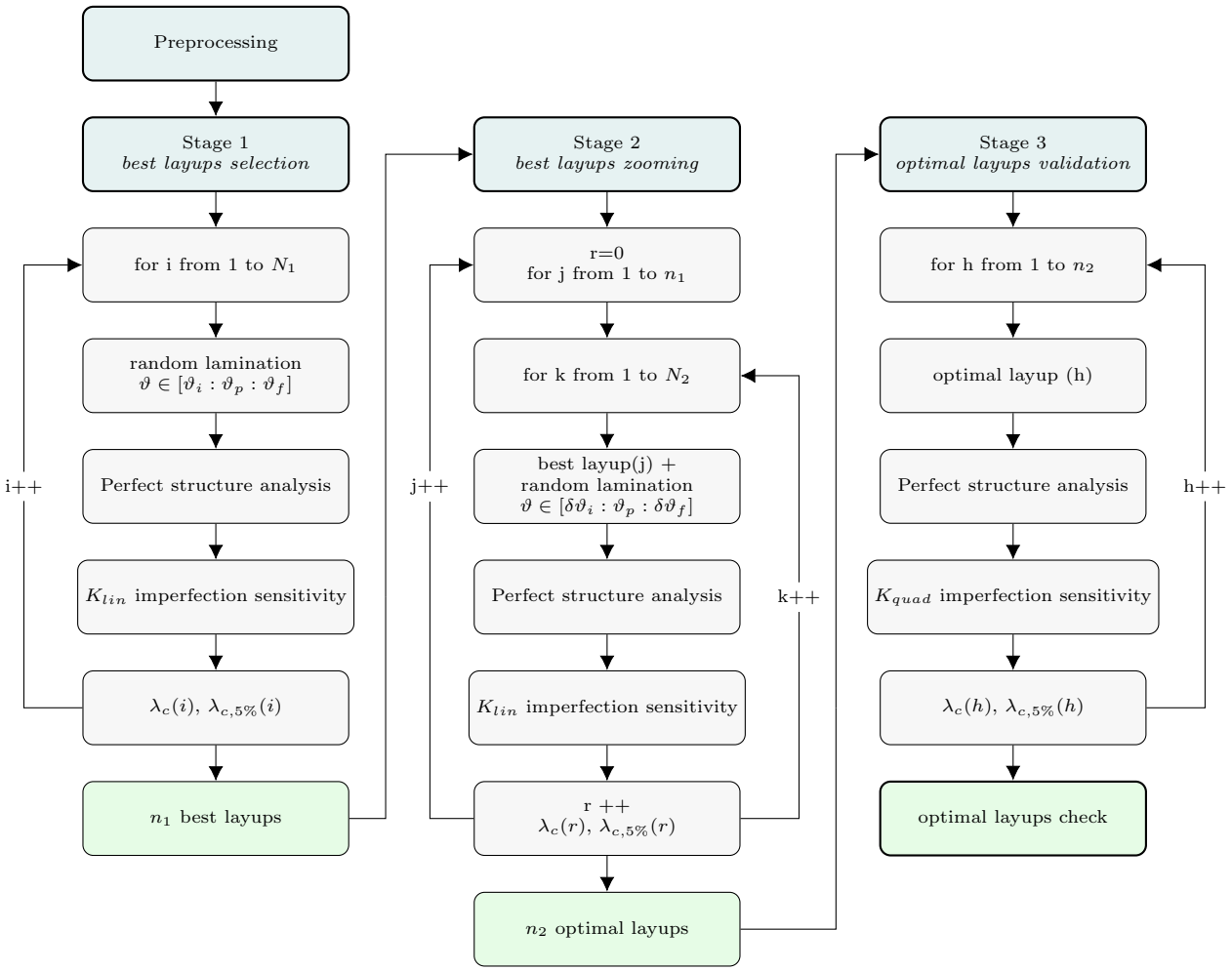

Figure 2: Diagram of the random scanning.

4. Numerical results

Two examples of stacking sequence optimisation based on the proposed strategy are presented in this section. In the first one, we look for the optimal values of two lamination parameters of a curved panel in compression and, due to the relatively small complexity of the problem, the uniform scanning approach is employed. The second test regards the optimisation of a stacking sequence defined by eight parameters, that is the fibre orientation of each layer, and the random scanning approach is used because of the extremely large number of possible layups. The capability of the proposed approach for describing the overall structural behaviour as well as to find optimal solutions can be seen, highlighting the strong influence of the lamination on the collapse load. Concerning the sensitivity analysis for the detection of the worst imperfection shape, the results provided by the Koiter method with the two a-posteriori account of the imperfections (K_{lin} and K_{quad}) are compared with the full FE solution (labelled as *Riks*) obtained using the standard arc-length method.

4.1. Curved panel in compression

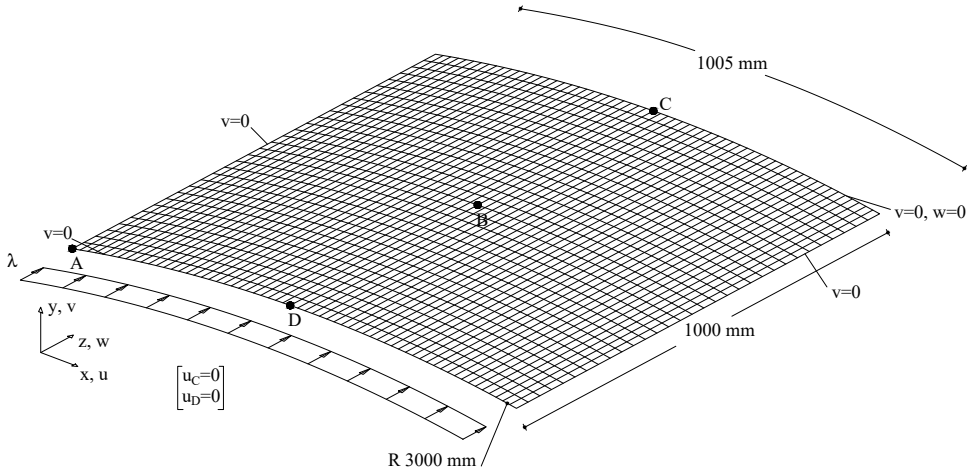

Figure 3: Curved panel: geometry and boundary conditions.

The test regards a curved cylindrical panel in compression. The geometry, the loads and the boundary conditions pictured in Fig.3 are related to the middle surface of the panel. The thickness of the shell is equal to $10\,mm$.

The properties of the material are $E_1 = 30.6\,GPa$, $E_2 = 8.7\,GPa$, $\nu_{12} = 0.29$, $G_{12} = 3.24\,GPa$, $G_{23} = 2.9\,GPa$. The panel is composed of six layers and the stacking sequence is $[\pm\vartheta_1, \pm\vartheta_2, \pm\vartheta_3]$, from inside-out and measured with respect to the 1-axis of the local reference system which is aligned with z. The structure is discretised by a mesh grid made of 60 solid-shell elements along the curved edges and 30 along the straight ones.

The optimisation problem consists in seeking the values of ϑ_1 and ϑ_3 which maximise the collapse load, while ϑ_2 is assumed constant and equal to $0°$.

The imperfection sensitivity analysis is carried out assuming random geometrical imperfections following the Monte Carlo method; the imperfections are generated as a linear combination of the displacement part of the buckling modes and uniformly distributed random numbers represent the coefficients of the combination. The resulting imperfection shape is scaled in order to have a maximum component equal to 0.1 of the thickness.

The space of the sought angles is uniformly scanned from $-90°$ to $90°$ every $18°$. The details of the two stages of the analysis are summarised in Table 1. The best 10 laminations detected in stage 1 are checked in

		stage 1	stage 2
	laminations	$N = 100$	$n = 20$
	ϵ_π tolerance	3/100	3/1000
	method	K_{lin}	K_{quad}
imperfections	starting	200	200
	increment	100	100
	maximum	2000	10000

Table 1: Curved panel: parameters of the Monte Carlo simulation.

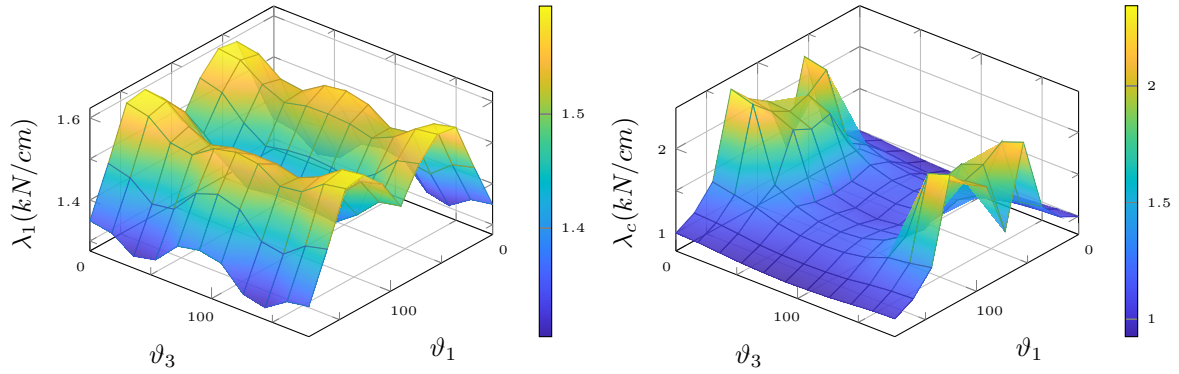

Figure 4: Curved panel: results of stage 1 in terms of first buckling load (left) and collapse load (right) trend with respect to the lamination angles.

stage 2. The same is done for the worst 10 laminations in order to show the great influence of the stacking sequence on the structural performances.

The number of significant buckling modes for the construction of the ROM generally changes with the lamination and cannot be imposed a-priori. In this respect, an adaptive criterion of selection is used. It consists in including the modes corresponding to critical loads that do not exceed 1.5 times the lowest one.

For the potential cases of stable post-critical behaviour, the deformation limit is reached when the displacement component w_A becomes greater than $2\,mm$.

Figure 4 shows, for stage 1, the trend of the first buckling load and of the collapse load in the angles domain. It can be observed that, as expected, the buckling load values are not directly linked to the collapse loads. It is worth noting that the unstable cases are the most frequent (darkest areas) and produce a low collapse load coincident with the limit load, while the maximum values (lighter areas) of the collapse load correspond to stable cases where the deformation limit dominates. In Fig.5 the collapse load is normalised with respect to the first eigenvalue, showing that the former is much lower then the second one for the unstable cases and confirming that the linearised buckling load is not a reliable objective function for the optimisation.

The best and the worst 10 cases, in terms of collapse load, are summarised in Table 2 for both stages. It highlights that stage 2 gives smaller collapse loads than stage 1 and that the number of imperfections significantly increases between the two stages due to the more restrictive values for the distribution parameters σ and μ adopted. The analysis shows also that the best stacking sequences detected at stage 1 are also the optimal ones of the stage 2. Note also that, as expected, the worst cases are symmetric with respect to the fibre direction and this confirms the robustness of the proposal in terms of number of numerical experiments. For example the layup $[0_4/\pm 72]$ gives identical results as $[0_4/\mp 72]$. For the stable cases, since the control point A is not located on the symmetry axis, the results in terms of collapse load are not symmetric unlike the linearised buckling loads. See for instance the layups $[\mp 54/0_4]$ and $[\pm 54/0_4]$.

The extreme cases are analysed more deeply in the following. The stacking sequence $[0_4/90_2]$ furnishes the worst results in terms of collapse load. For this lamination, the equilibrium paths corresponding to

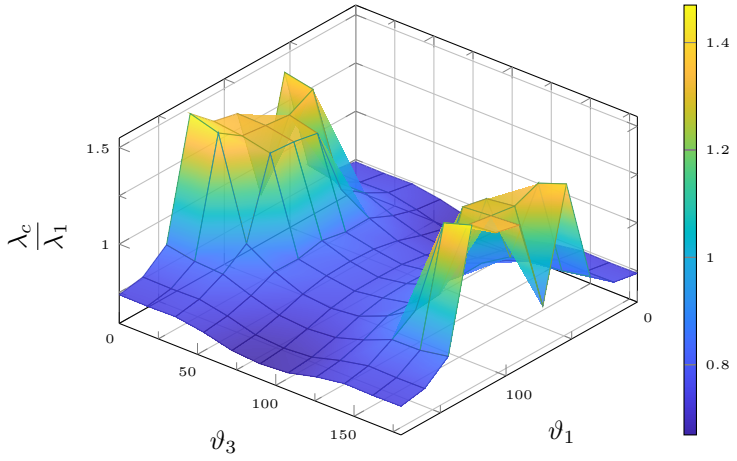

Figure 5: Curved panel: results of stage 1 in terms of collapse load normalised with respect to the first buckling load.

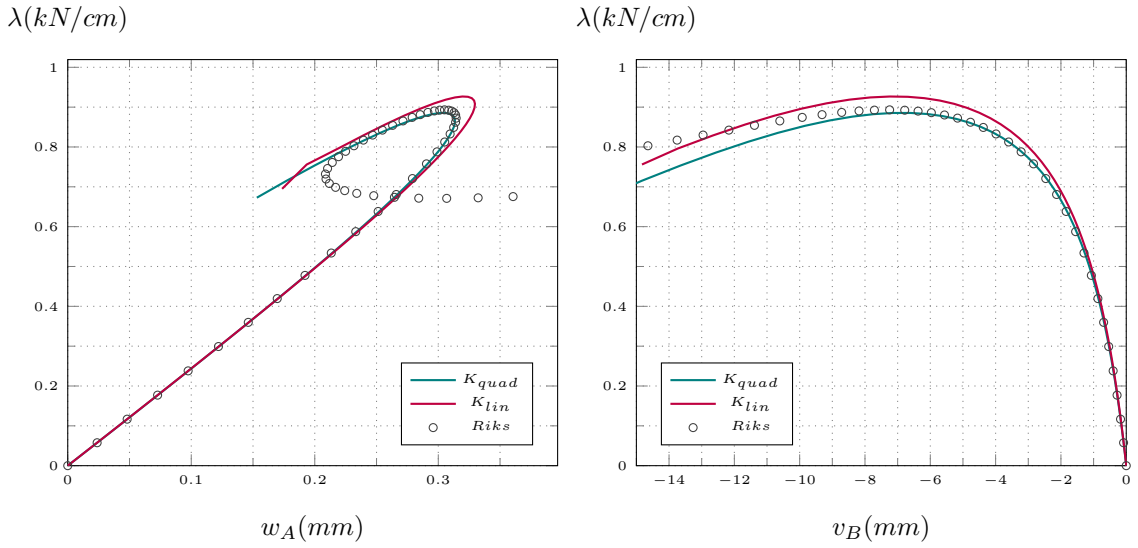

Figure 6: Curved panel: equilibrium path for the worst imperfection shape in stage 2, path following vs Koiter a-posteriori, lamination $[0_4/90_2]$.

lamination	buckling loads			Stage 1			Stage 2		
	λ_1	λ_2	λ_3	λ_c	$\frac{\lambda_c}{\lambda_1}$	N_i	λ_c	$\frac{\lambda_c}{\lambda_1}$	N_i
$[\mp 54/0_4]$	1.595	1.986	-	2.344	1.470	500	2.354	1.476	2797
$[\mp 54/0_2/\pm 18]$	1.587	1.971	-	2.265	1.427	500	2.304	1.452	1599
$[\mp 54/0_2/\mp 18]$	1.587	1.975	-	2.260	1.424	499	2.294	1.445	1698
$[\pm 54/0_4]$	1.595	1.986	-	2.245	1.408	500	2.277	1.428	1699
$[\pm 54/0_2/\pm 18]$	1.587	1.975	-	2.187	1.377	500	2.228	1.404	1699
$[\pm 54/0_2/\mp 18]$	1.587	1.971	-	2.148	1.354	500	2.215	1.396	1298
$[\mp 72/0_4]$	1.548	1.993	-	2.107	1.361	500	2.172	1.403	2100
$[\mp 72/0_2/\pm 18]$	1.535	1.966	-	2.061	1.343	500	2.122	1.383	1597
$[\mp 72/0_2/\mp 18]$	1.533	1.969	-	2.060	1.343	600	2.127	1.387	1600
$[\pm 72/0_2/\pm 18]$	1.533	1.969	-	2.014	1.314	600	2.074	1.353	1500
$[0]_6$	1.350	1.978	-	0.996	0.738	352	0.970	0.719	1499
$[0_4/\pm 18]$	1.340	1.938	-	0.987	0.736	466	0.966	0.720	2974
$[0_4/\mp 18]$	1.340	1.938	-	0.987	0.736	585	0.966	0.720	2064
$[0_4/\pm 36]$	1.305	1.799	-	0.965	0.740	493	0.945	0.724	2385
$[0_4/\mp 36]$	1.305	1.799	-	0.965	0.740	493	0.945	0.724	1791
$[0_4/\pm 54]$	1.317	1.661	-	0.944	0.717	500	0.910	0.691	3391
$[0_4/\mp 54]$	1.317	1.661	-	0.944	0.717	800	0.910	0.691	4679
$[0_4/\mp 72]$	1.371	1.632	2.022	0.933	0.680	500	0.894	0.652	2498
$[0_4/\pm 72]$	1.371	1.632	2.022	0.933	0.680	700	0.893	0.652	2100
$[0_4/90_2]$	1.382	1.628	1.962	0.925	0.669	500	0.885	0.641	2499

Table 2: Curved panel: results of the best 10 and the worst 10 laminations. The loads are expressed in kN/cm.

the worst imperfection shape are reported in Fig.6 using the Koiter method, with both K_{lin} and K_{quad} approaches, and a path-following strategy. The solution found by K_{quad} is in accordance with the one of the path following analysis on the full FE model and, in particular, the collapse load is accurately predicted. Conversely, the cheaper approach K_{lin} gives a slightly higher value of the collapse load but is however able to capture the structural behaviour. The buckling modes and the quadratic correctives used in the Koiter analysis for building the ROM of the corresponding perfect structure are pictured in Fig.7 while Fig.8 and Fig.9 show the deformed configuration at collapse load and the worst imperfection shape, respectively. It is interesting to note as the worst imperfection shape does not correspond, in this case, to the first buckling mode and as all the buckling modes contribute to the deformed shape at the limit point.

To point out the influence of the number of buckling modes included in the ROM on the collapse load, an imperfection sensitivity analysis with 3 modes, that is the number used during the scan process, and 8 modes has been carried out for the case $[0_4/90_2]$. The minimum collapse load and its 5% fractile provided when increasing the imperfections has been monitored. The results are pictured in Fig.10. The collapse load from the two cases stabilises at the same value although when 3 modes are employed it converges for a smaller number of imperfections. On the contrary, as expected, the fractiles are quite different because, by enlarging the number of the modes, the space of the possible imperfections also increases without providing any further information about the worst imperfection, which is well represented by the first 3 modes.

Moreover, for a fixed number of modes, the frequency distribution converges quickly. This can be seen in Fig.10 where the fractile does not change significantly, or in Fig.11 and Table 3 which show, for 8 modes, how the probability density function and the parameters of the distribution vary with the number of imperfections.

The other extreme lamination is $[\mp 54/0_4]$, characterised by a stable post critical behaviour and the highest collapse load. In Fig.13, the corresponding equilibrium paths traced by Koiter (ROM) and Riks (full FE model) analyses are reported showing a good agreement. The deformed configuration at the last evaluated equilibrium point is shown as well. The buckling modes and the corresponding corrective modes used to construct the ROM are pictured in Fig.14. Finally, to assess the choice of discretising the angles domain by 18°, the optimisation process is repeated with a finer discretisation of 6°. In this case, the method finds $[\mp 48/0_4]$ as the best layup with a collapse load $\lambda_c = 2,369$. The solution is just slightly better than that provided by the previous analysis, confirming that 18° was already a good choice.

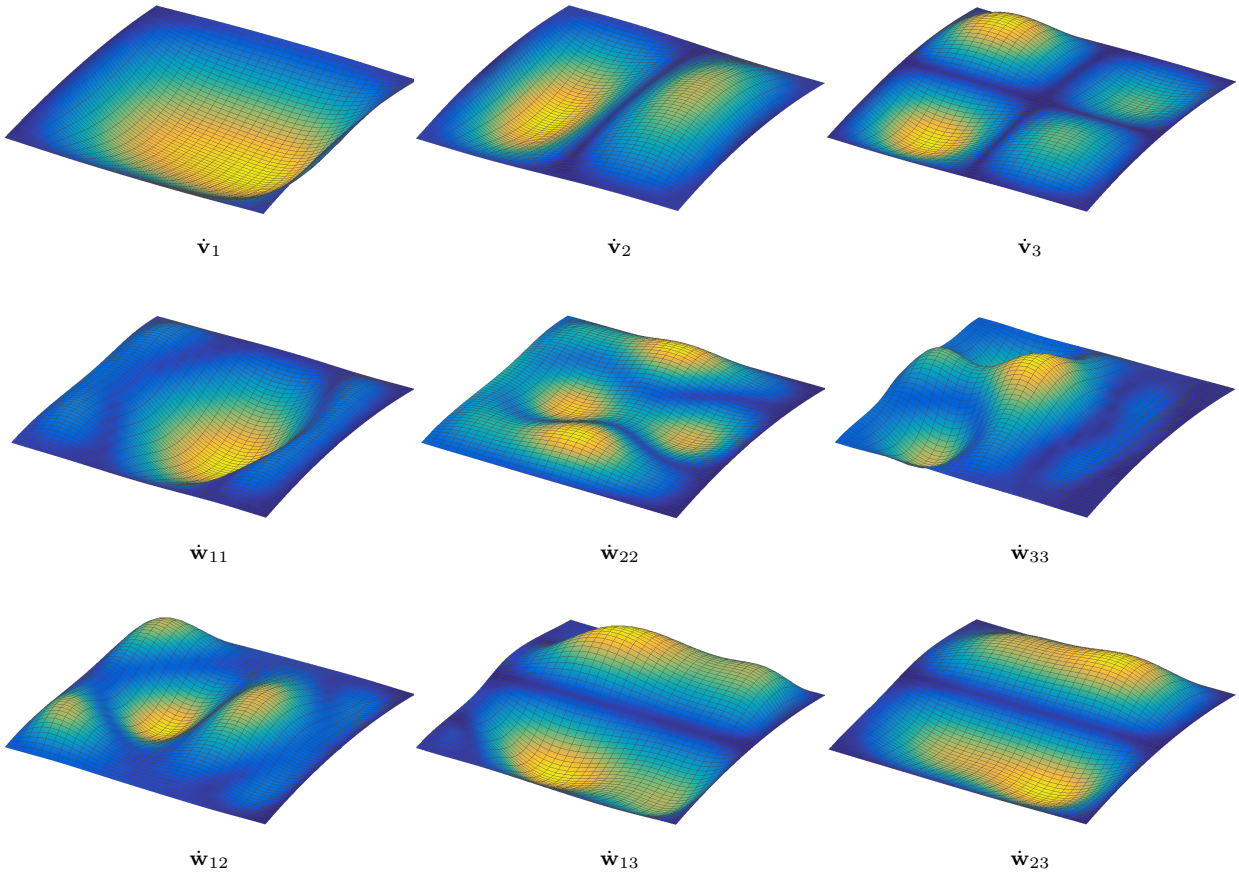

Figure 7: Curved panel: buckling modes and quadratic correctives, case $[0_4/90_2]$.

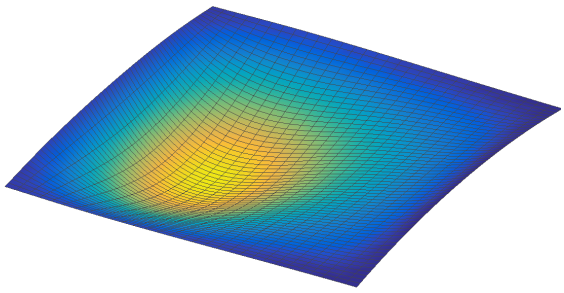

Figure 8: Curved panel: deformed shape at collapse point, case $[0_4/90_2]$.

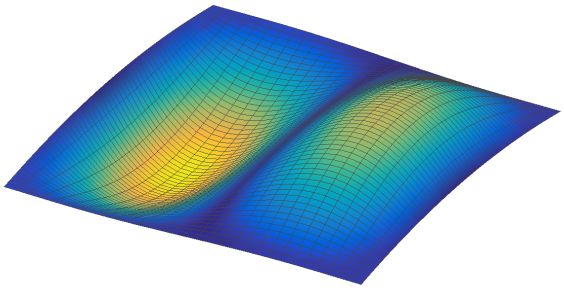

Figure 9: Curved panel: worst imperfection shape, lamination $[0_4/90_2]$.

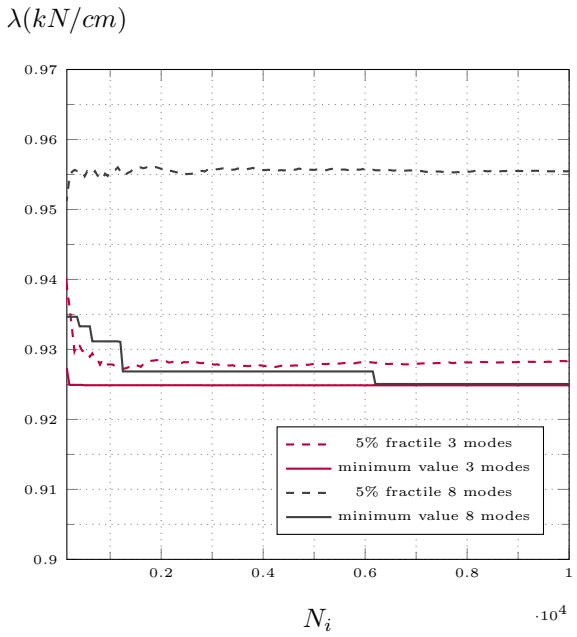

Figure 10: Curved panel: 5% fractile and minimum value of the collapse load versus number of imperfections for 3 and 8 modes, case $[0_4/90_2]$.

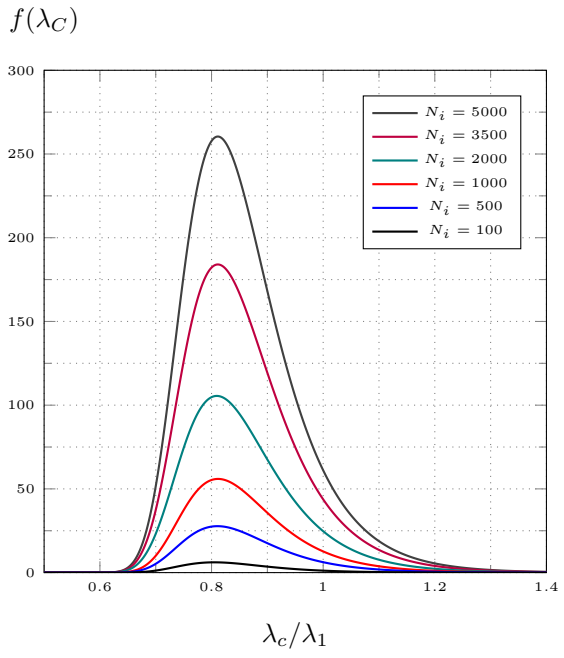

Figure 11: Curved panel: Gumbel max probability density function for different number of imperfections, lamination $[0]_6$, 8 modes.

N_i	μ	σ
100	-0.8049	0.0755
500	-0.8105	0.0788
1000	-0.8116	0.0786
2000	-0.8094	0.0809
3500	-0.8113	0.0806
5000	-0.8113	0.0801

Table 3: Curved panel: distribution parameters variation with the number of imperfections, lamination $[0]_6$.

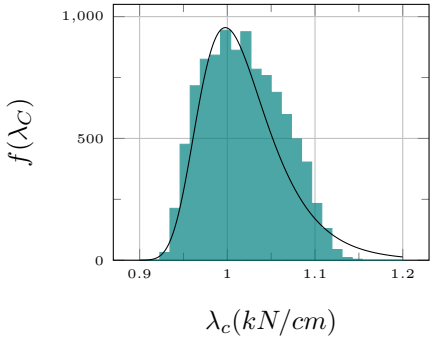

Figure 12: Curved panel: frequencies of the collapse load, lamination $[0_4/90_2]$, 8 buckling modes, 10000 imperfections.

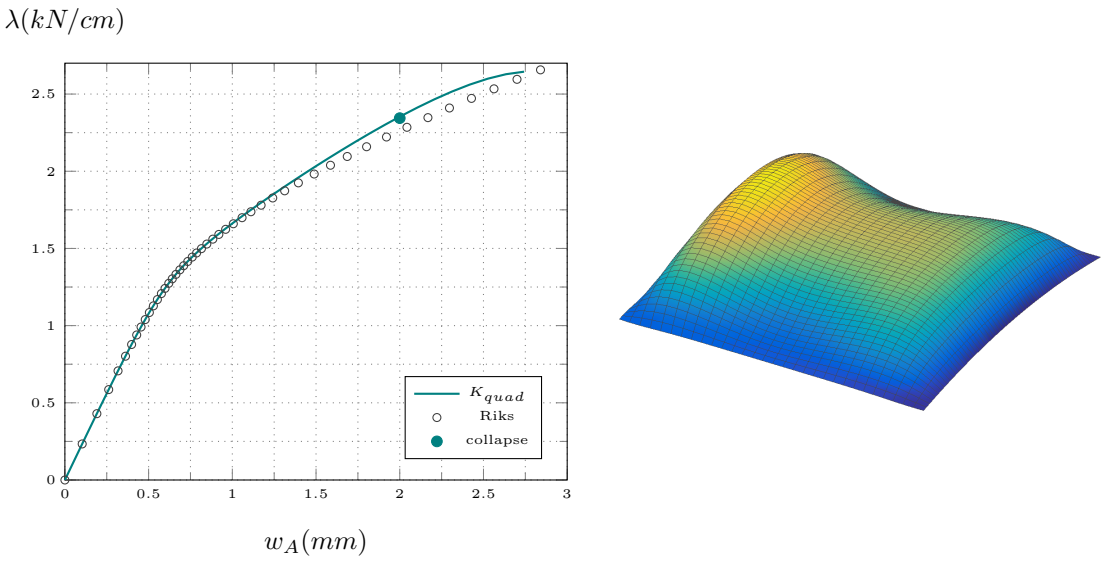

Figure 13: Curved panel: equilibrium path (left) and deformed shape at the last evaluated equilibrium point (right), lamination $[\mp 54/0_4]$.

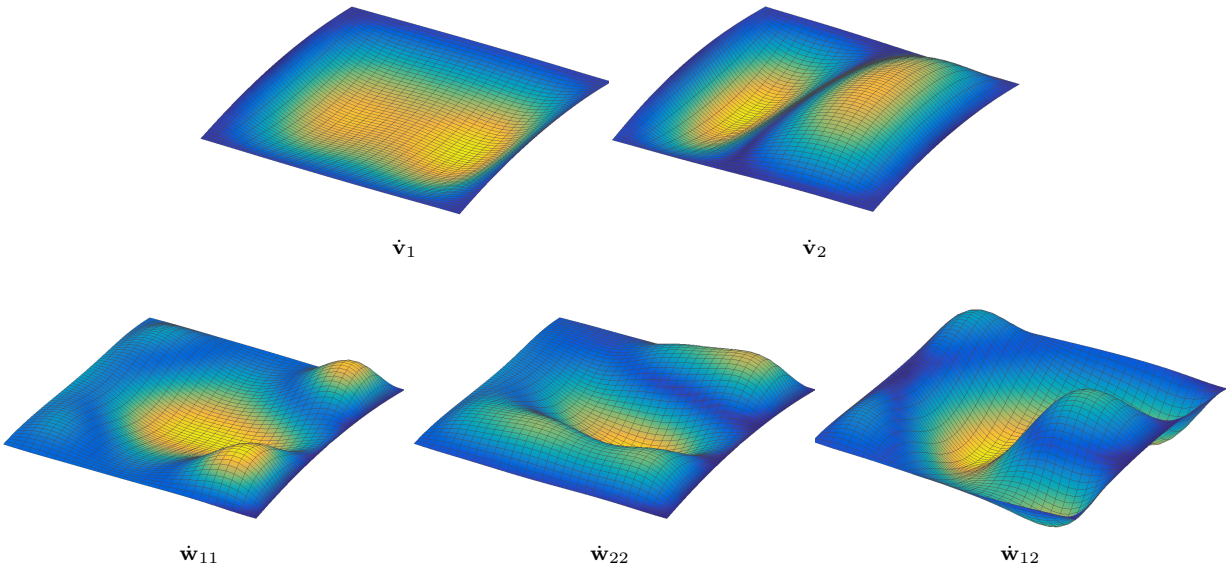

Figure 14: Curved panel: buckling modes and quadratic correctives for the case $[\mp 54/0_4]$.

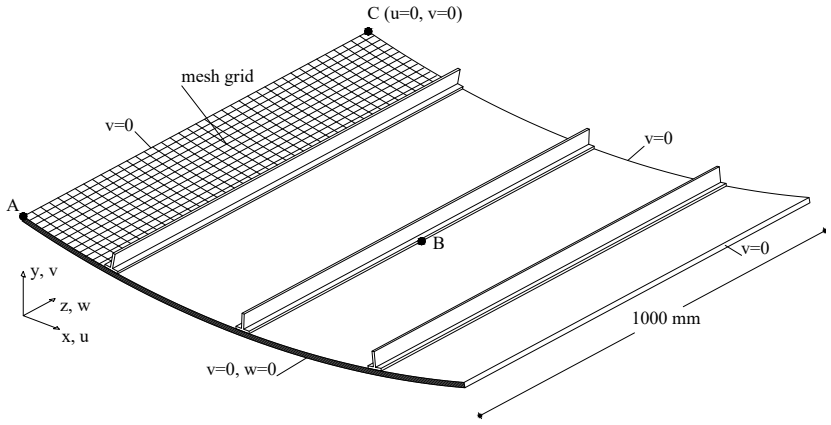

Figure 15: Stiffened panel: geometry and boundary conditions.

4.2. Stiffened panel

The second test regards a curved panel with "T" stiffeners in compression, like those commonly employed for aeronautical structures [8]. In Fig.15 an axonometric projection shows the geometry and the boundary conditions, while geometrical details of a section have been pictured in Fig.16. The v displacement of the lateral faces of the four panels is bounded and the deformation of only one curved edge is constrained, also along z. In the illustrations, it is possible to see the mesh grid details for the 3D solid-shell description of the structure. It is worth noting how the solid-shell finite element allows us to model, easily and accurately, the connection between the panel and the stiffeners, with no need for rigid links or offsets, in contrast to classical shell models. The curved faces and the stiffener ends are loaded by a uniform line load $\lambda = 1$.

The same material is employed for the skin and the stiffeners and it is characterised by $E_1 = 30.6\,GPa$, $E_2 = 8.7\,GPa$, $\nu_{12} = 0.3$, $G_{12} = 3.4\,GPa$, $G_{23} = 2.9\,GPa$, with respect to the local reference system which has the direction 1 aligned with the global direction z while the direction 3 is along the normal at the middle plane of the skin. The stiffener lamination is supposed to be constant and equal to $0°$, while eight layers define the lamination of the skin labelled as $[\vartheta_1/\ldots/\vartheta_8]$ where every ϑ_i is a multiple of $18°$ and can vary from $-90°$ to $90°$. The purpose of the test is studying the variability of the post-critical behaviour when the lamination changes and seeking the laminations with the maximum collapse load. The solutions with minimum collapse load are searched as well, just to identify the range of variability of the structural performances. The collapse load for the stable configurations is the load producing the deformation limit $w_A = 4\,mm$. As in the first test, the buckling modes employed for the ROM of the Koiter analyses correspond to buckling loads which do not exceed 1.5 times the first one.

The parameters used to set up the three stages of the random scanning approach are reported in Table 4. In the first stage, $N_1 = 2500$ random uniformly generated laminations are analysed and the $n_1 = 10$ best and the 10 worst laminations (in terms of collapse load), reported in Table 5, are selected. In the second stage, for each of these configurations, a further $N_2 = 100$ randomly generated laminations are considered with each layer angle that can vary between $-36°$ and $36°$ with an increment of $18°$ with respect to the likely optimal values identified by the first stage. Lastly, in stage 3 the best $n_2 = 10$ and the worst 10 results obtained in stage 2, and labelled as indicated in Table 6, are analysed using the accurate account of geometrical imperfections and a more restrictive tolerance for parameters μ and σ; a summary of the results is reported in Table 7.

Even though the number of finite element parameters is quite significant, the code is not really time consuming. For instance, the average time taken by a prototype code for analysis each layup at stage 1 is 32.02 seconds (i7-6700HQ CPU 2.6Ghz, Matlab R2016a, single core) considering that the average number of imperfections per layup is 805.

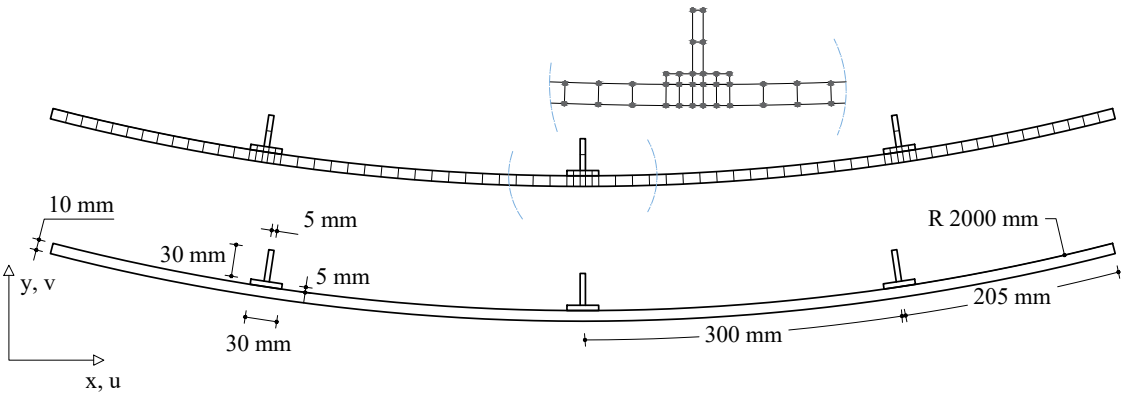

Figure 16: Stiffened panel: section geometry and mesh.

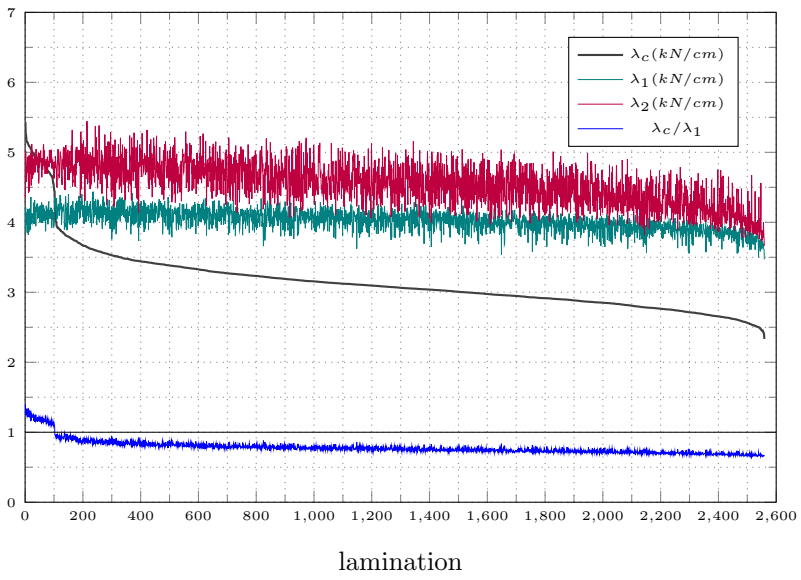

Figure 17: Stiffened panel: collapse load and buckling loads for the lamination in order of decreasing collapse load, stage 1.

		stage 1	stage 2	stage 3
	laminations	2500	2000	20
	tolerance	3/100	5/1000	3/1000
	method	K_{lin}	K_{lin}	K_{quad}
	starting	50	200	200
imperfections	increment	50	50	100
	maximum	2000	2000	10000

Table 4: Stiffened panel: parameters of the Monte Carlo simulation.

lamination	λ_1	λ_2	λ_c	$\lambda_{c,5}$	λ_c/λ_1	N_i
$[18/36/-18/72/0_4]$	3.8805	4.3430	5.4337	-	1.4003	350
$[-72/36/72/-18/0/72/0/-18]$	4.2127	5.0184	5.2665	-	1.2501	350
$[-72/36/-18/-36/18/0/-18/0]$	3.9662	4.8839	5.2580	-	1.3257	200
$[-54_2/0/-36/-18/0/18/0]$	3.8521	4.7065	5.1439	-	1.3354	350
$[90/-72/0/18_2/0/-18/0]$	3.8604	4.7119	5.0942	-	1.3196	550
$[54_2/18/0/54/0/-18/0]$	3.8930	4.7015	5.0641	-	1.3008	300
$[72/-54/72_2/0/-72/0_2]$	4.3619	4.9789	5.0532	-	1.1585	350
$[36/54/-72/18/36/0_2/-18]$	4.0863	4.7736	4.9990	-	1.2234	400
$[72/-54/36/18/-36/18/0_2]$	4.0992	4.9873	4.9985	-	1.2194	300
$[54/72/0/72/36/0_2]$	3.9844	4.6742	4.9831	-	1.2506	250
$[-18/-36/-18/-36_2/72/-72/90]$	3.6837	3.7316	2.4582	2.4614	0.6673	300
$[-18/0/18/90_2/-54_2/-72]$	3.6686	3.7659	2.4519	2.4539	0.6683	250
$[0_2/-54/72_2/-54/72/-72]$	3.7314	3.7613	2.4511	2.4534	0.6569	300
$[18_2/-72_2/36/-54/54_2]$	3.6627	3.8805	2.4505	2.4525	0.6690	300
$[18_2/-36/-72/-54/-72/90/-54]$	3.6901	3.7830	2.4503	2.4525	0.6640	400
$[-18_2/54/-72/-54/72/90/-72]$	3.6955	3.8094	2.4295	2.4316	0.6574	400
$[0/-54/-72_2/(-54/90)_2]$	3.6464	3.9985	2.4255	2.4286	0.6652	250
$[18/-18/54_2/-72_3/-54]$	3.6160	3.8386	2.4211	2.4234	0.6696	300
$[0/18/-36/-72/54_2/90/72]$	3.6131	3.7729	2.4016	2.4048	0.6647	450
$[18_2/0/36/54/72/54/72]$	3.4698	3.6626	2.3334	2.3359	0.6725	250

Table 5: Stiffened panel: results of the best 10 and the worst 10 laminations, stage 1. The loads are expressed in kN/cm.

The curves in Fig.17 plot the collapse load, the two lowest buckling loads λ_1 and λ_2 and the ratio between the collapse load and the first eigenvalue as a function of a lamination index. This is an integer number which is assigned to each lamination after they are ordered in terms of decreasing collapse load. The laminations with the smallest index have a stable behaviour and collapse for reaching the deformation limit. The buckling loads in these cases are well separated from each other. The first buckling load is actually quite constant with the lamination though, when the second one gets closer to it, the collapse load, due to modal interaction phenomenon, drastically reduces. This behaviour is significantly more evident in Fig.18 where the results of stage 2 are reported. The best laminations in terms of collapse load are characterised by an evident distance between the first and the second linearised buckling load and exhibit a stable behaviour. Conversely, for the worst laminations, the second eigenvalue is very close to the first one and the modal interaction leads to a relevant unstable behaviour with an imperfection sensitive limit load.

Some equilibrium paths are presented in Fig.19. The collapse loads predicted by the Koiter method are practically coincident with those provided by the Riks analysis with the full FE model. The buckling modes used in the ROM and some quadratic correctives are pictured in Fig.20 and in Fig.23 for the laminations L1 and L20 respectively. In addition, Fig.21 shows the worst imperfection shape detected in stage 2 for the lamination L20 and the corresponding deformed shape at the limit point is reported in Fig.22. The convergence of the Monte Carlo optimisation is shown in Fig.24, that is the trend of the maximum and the minimum collapse load for an increasing number of analysed laminations. In particular, a little over a thousand of layups has to be considered to obtain a converged value of the maximum collapse load. Lastly, Fig.25 indicates how the structural behaviour in terms of equilibrium path drastically changes with the

stacking sequence and, in particular, how the post-critical behaviour varies from strongly unstable to stable, confirming again the great influence of a stacking sequence optimisation.

label	lamination
L1	$[-72/18/-18_2/0/18/0_2]$
L2	$[72/0/-18/-36/0_2/-18/0]$
L3	$[-72/18/72/-18/18/72/0_2]$
L4	$[-54/0/-18/-72/18/0_2/18]$
L5	$[-72/54/-36/0/18/0_2/18]$
L6	$[-72/-18/36/0/-72/0_2/18]$
L7	$[0/72/-18/36/18/0/18/0]$
L8	$[90/18/0/-18/18_2/-18/0]$
L9	$[72/18/-54/18/0_2/36/0]$
L10	$[-72/54/0/-36/(0/18)_2]$
L11	$[0/-54_4/90/-72/-54]$
L12	$[0_2/-72/90/-72/-54/-72/90]$
L13	$[-18/0/72_2/90/54/72_2]$
L14	$[-18_2/72_2/-72/90/-54_2]$
L15	$[-18_2/72/90_3/-72/-54]$
L16	$[18/-72/-54/-72_2/90/-72]$
L17	$[0/18/54_2/72/90/-72/72]$
L18	$[0/-18/-54_2/90/-72/90/72]$
L19	$[-18_2/36/-72/-54/90/72_2]$
L20	$[0_2/54/72_2/90_2/72]$

Table 6: Stiffened panel: labels of the best 10 and the worst 10 laminations, stage 2.

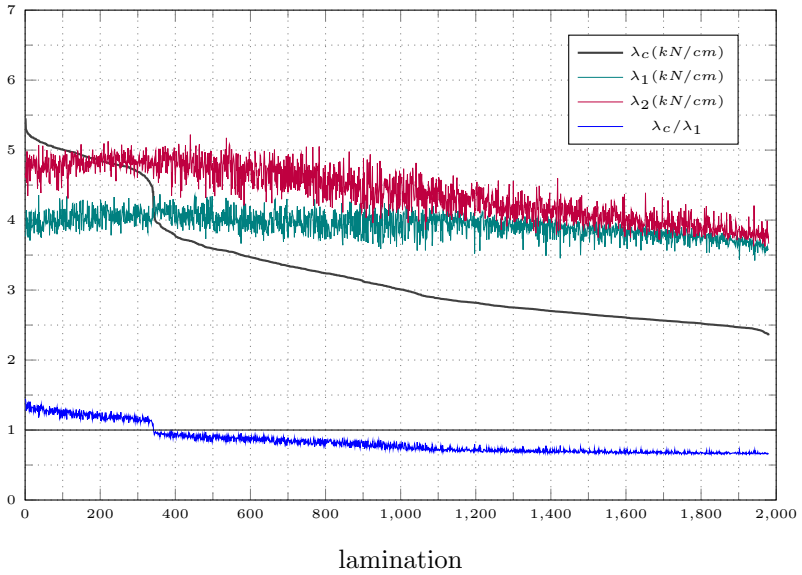

Figure 18: Stiffened panel: collapse load, fractile and buckling loads for the lamination in order of decreasing collapse load, stage 2.

	buckling loads				Stage 2			Stage 3		
	λ_1	λ_2	λ_3	λ_4	λ_c	$\frac{\lambda_c}{\lambda_1}$	N_i	λ_c	$\frac{\lambda_c}{\lambda_1}$	N_i
L1	3.771	4.663	5.610	-	5.450	1.442	850	5.463	1.449	1200
L2	3.801	4.605	5.645	-	5.302	1.395	1100	5.314	1.398	2200
L3	4.140	4.823	5.975	-	5.289	1.276	600	5.300	1.280	2500
L4	3.876	4.534	5.713	-	5.277	1.361	900	5.286	1.364	2100
L5	4.016	4.982	5.786	-	5.260	1.310	600	5.250	1.307	2200
L6	4.025	4.762	5.826	-	5.254	1.306	950	5.260	1.307	1700
L7	3.785	4.344	5.644	-	5.238	1.384	700	5.244	1.386	3600
L8	3.752	4.615	5.573	-	5.236	1.396	800	5.242	1.397	1600
L9	3.956	4.781	5.713	-	5.229	1.322	950	5.238	1.324	800
L10	3.971	4.891	5.720	-	5.227	1.316	950	5.240	1.320	1400
L11	3.587	3.864	5.110	5.305	2.389	0.666	750	2.381	0.664	2300
L12	3.550	3.809	5.000	5.111	2.387	0.672	800	2.380	0.670	2598
L13	3.562	3.835	5.111	5.131	2.387	0.670	1000	2.380	0.668	2200
L14	3.618	3.752	5.238	5.341	2.382	0.658	750	2.374	0.656	1800
L15	3.618	3.765	5.195	5.343	2.381	0.658	1100	2.373	0.656	1400
L16	3.563	3.992	5.184	5.220	2.378	0.667	500	2.373	0.666	2300
L17	3.621	3.757	5.116	5.255	2.380	0.657	700	2.369	0.654	1400
L18	3.585	3.744	5.058	5.269	2.373	0.662	650	2.364	0.659	1900
L19	3.579	3.774	5.153	5.289	2.371	0.662	750	2.362	0.660	1600
L20	3.579	3.663	4.967	5.140	2.353	0.658	900	2.345	0.655	1500

Table 7: Stiffened panel: stage 2 and stage 3 results. The loads are expressed in kN/cm.

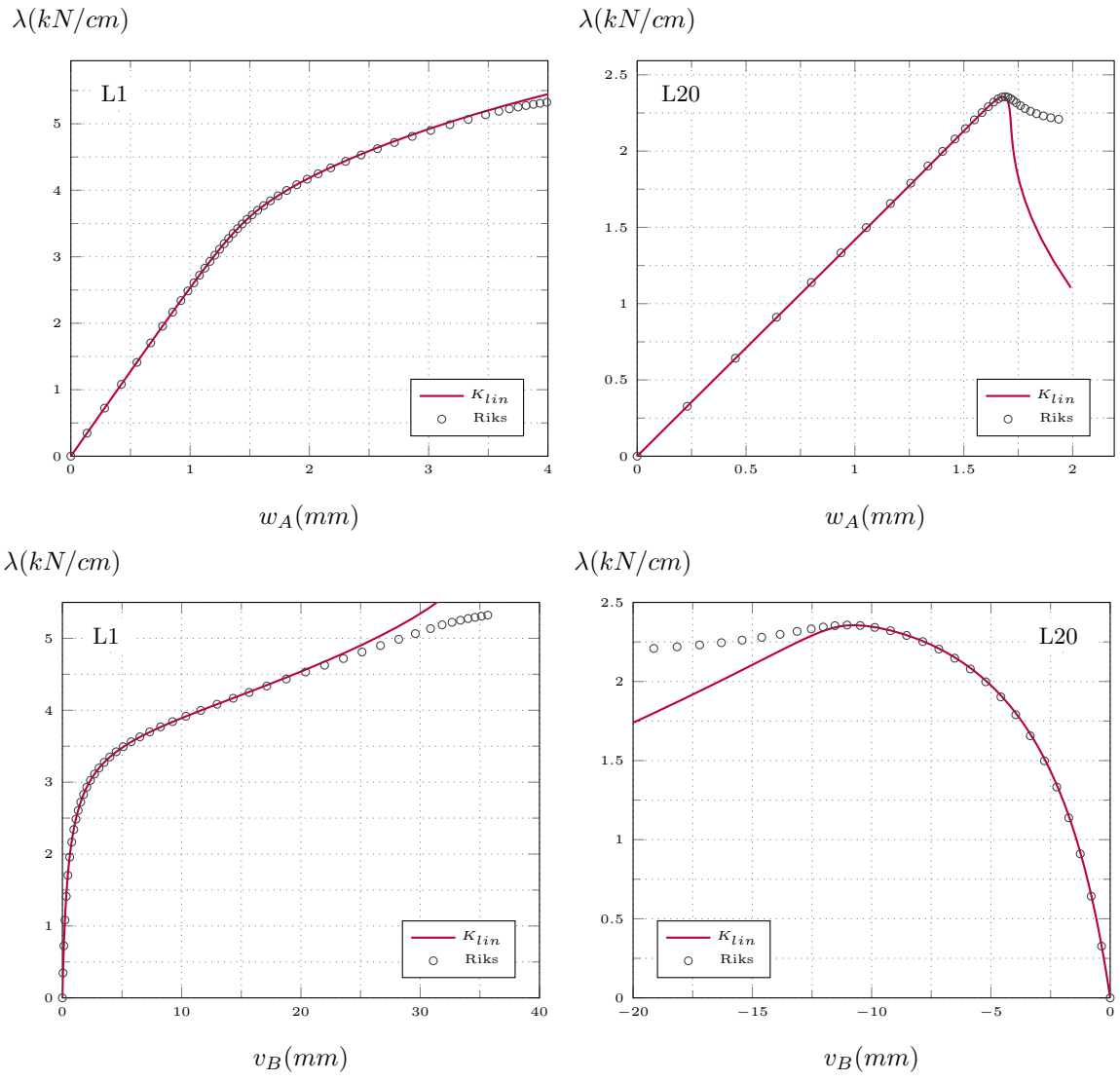

Figure 19: Stiffened panel: equilibrium paths for the worst imperfection shape and laminations L1 and L20, path following vs Koiter.

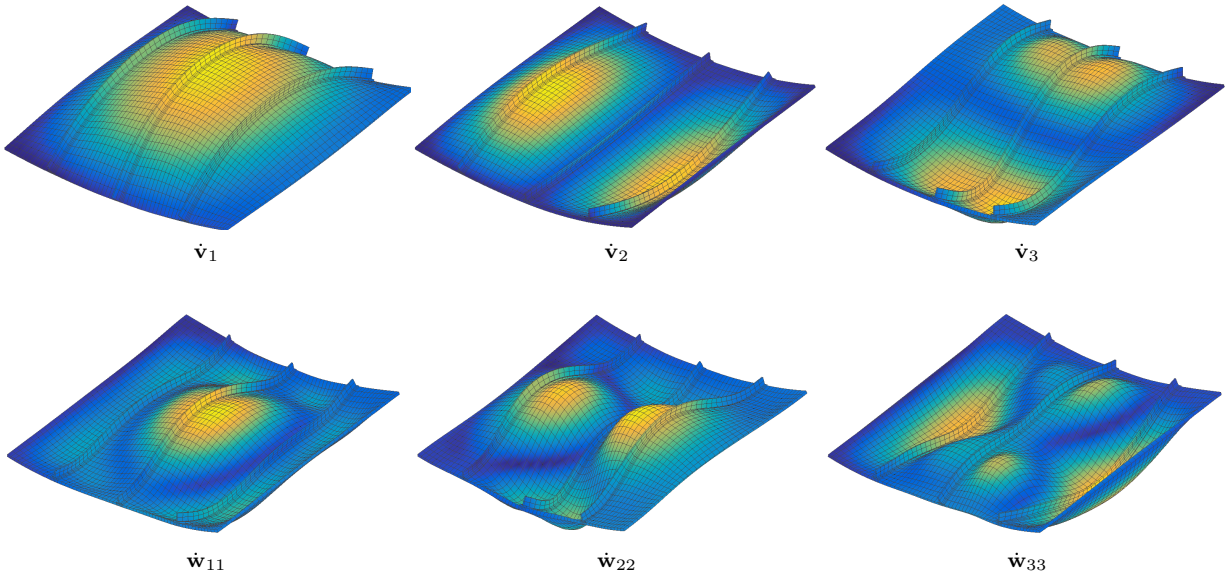

Figure 20: Stiffened panel: buckling modes and quadratic correctives, case L1.

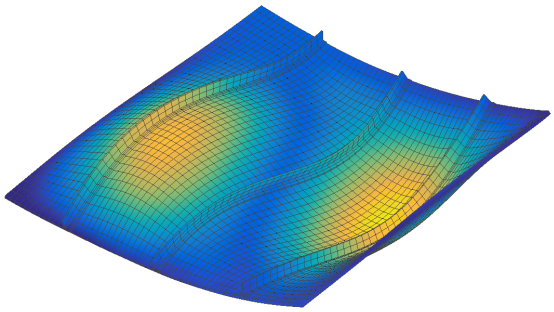

Figure 21: Stiffened panel: worst imperfection shape, L20.

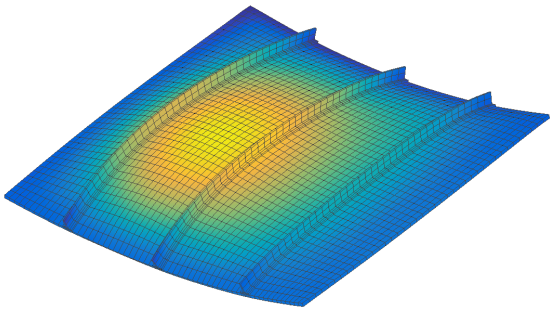

Figure 22: Stiffened panel: deformed shape at collapse point, L20.

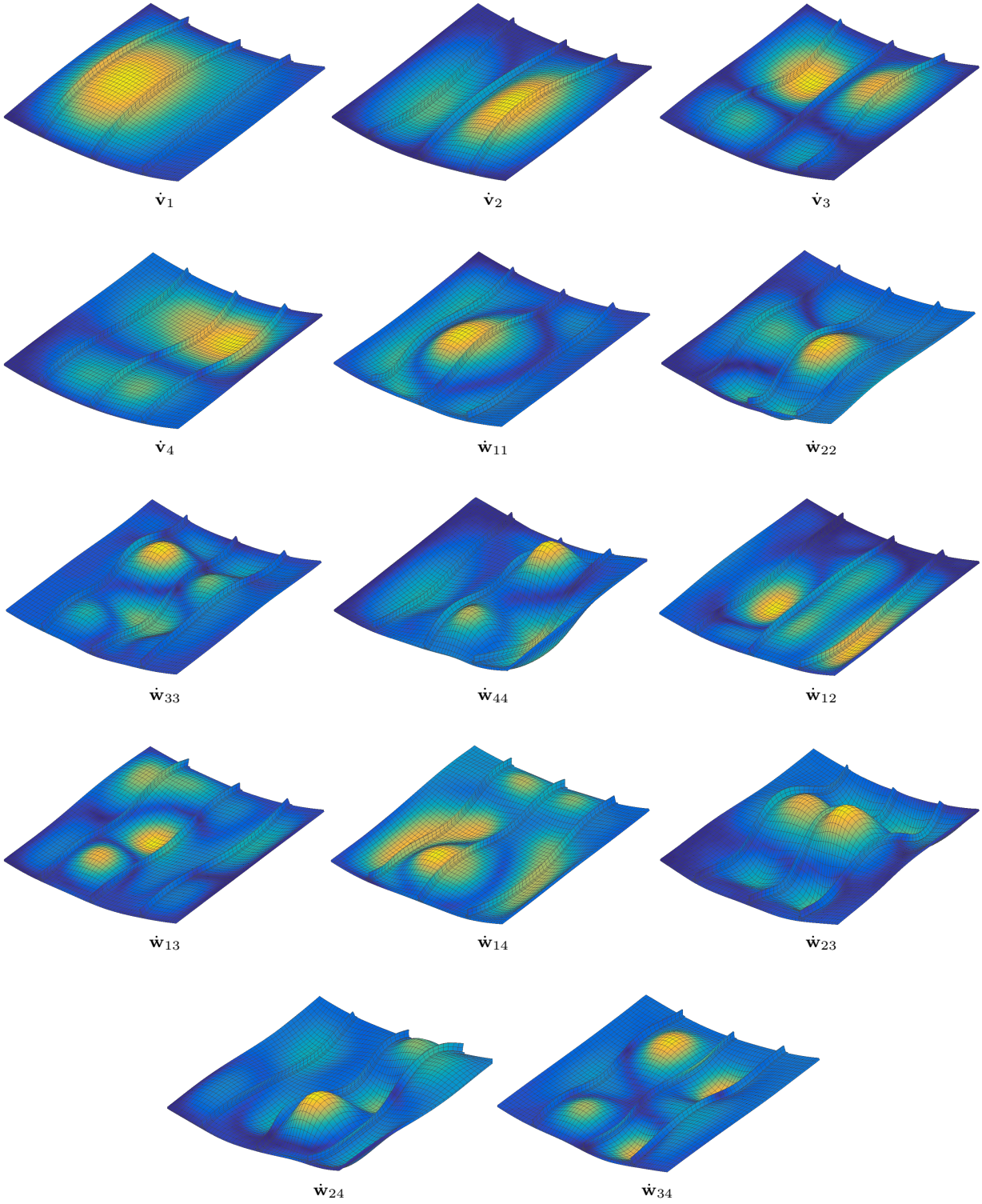

Figure 23: Stiffened panel: buckling modes and quadratic correctives, case L20.

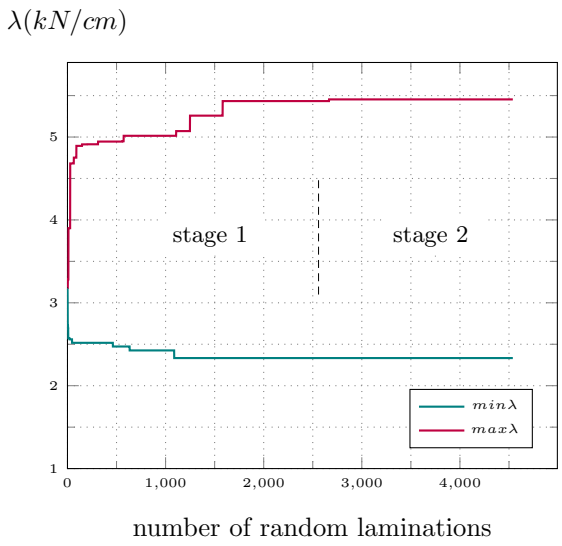

Figure 24: Stiffened panel: maximum and minimum collapse loads when the laminations increase.

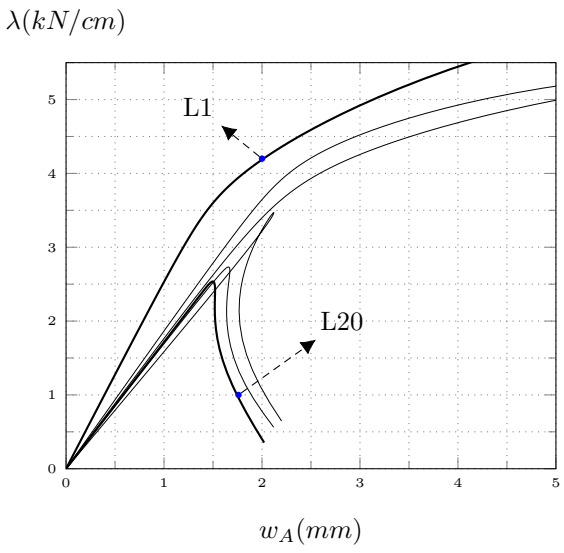

Figure 25: Stiffened panel: equilibrium paths for some laminations at stage 2.

5. Conclusions

A strategy completely based on stochastic simulations for optimising the stacking sequence of slender composite shells undergoing buckling was presented in this paper. The objective function is the collapse load, evaluated by taking into account the initial post-buckling behaviour. The main idea consists in the use of random numerical experiments for detecting both the best layup and the worst shape of the geometrical imperfection. A solid-shell finite element model was adopted to describe the structural problem accurately with no limitation on geometry, material configuration and boundary conditions. Generally, the discrete problem is governed by a significant number of degrees of freedom, which makes the Monte Carlo optimisation prohibitive. For this reason, the FE unknowns were replaced, for each random layup by a reduced order model built, according to the multimodal Koiter method, starting from the initial path tangent and a few buckling modes associated to the first eigenvalues of a linearised buckling analysis. The ROM, governed by a few modal amplitudes, made it possible, for each material configuration, to quickly predict the initial post-buckling path of the perfect structure with a high accuracy in both stable and limit point situations, including the modal interaction phenomenon. Moreover, the safest collapse load of each stacking sequence, corresponding to the worst imperfection shape, was estimated by means of a Monte Carlo imperfection sensitivity analysis, that is the evaluation of the equilibrium path for thousands of imperfections. This part, that is usually quite time consuming, was made really inexpensive by including the effects of the imperfections directly in the ROM of the perfect structure. The number of imperfections to consider was controlled by checking the convergence of the parameters of the Gumbel-max distribution, which represents the probability density function of the collapse load well.

Two examples of layup optimisation regarding curved multi-layered panels, with and without stiffeners, were reported. In the first one, the stacking sequence was expressed in terms of two parameters. In this case, the great efficiency of the Koiter method made it possible to uniformly scan the entire population of stacking sequences. In the second one, the fibre orientation of each of the eight layers was chosen as an independent parameter. The complexity of the problem was handled by means of the more general random search and it was shown that a converged value of the maximum collapse load is obtained with a thousand random layups. The numerical results confirm the importance of correct design of the stacking sequence, which should take account of the post-critical behaviour to maximise the collapse load. The optimisation led to a drastic change in structural behaviour, which ranges from unstable and sensitive to imperfections to stable without imperfection sensitivity. The examples showed that, on the contrary, the smallest linearised buckling load cannot be used as objective function for the optimisation as it can generally be quite different from the collapse load, especially in the case of modal interaction. This is evident in the second test proposed where the first buckling load is practically constant with the lamination while the collapse load changes significantly.

Acknowledgement

The research leading to these results has received national funding from MIUR-PRIN project: " *Advanced mechanical modeling of new materials and structures for the solution of 2020 Horizon challenges*".

References

References

[1] Z. Wu, G. Raju, P. M. Weaver, Optimization of postbuckling behaviour of variable thickness composite panels with variable angle tows: Towards "buckle-free" design concept, International Journal of Solids and Structures (2017). doi:https://doi.org/10.1016/j.ijsolstr.2017.08.037.

[2] G. Zucco, R. Groh, A. Madeo, P. Weaver, Mixed shell element for static and buckling analysis of variable angle tow composite plates, Composite Structures 152 (Supplement C) (2016) 324 – 338. doi:https://doi.org/10.1016/j.compstruct.2016.05.030.

[3] B. Wang, K. Tian, C. Zhou, P. Hao, Y. Zheng, Y. Ma, J. Wang, Grid-pattern optimization framework of novel hierarchical stiffened shells allowing for imperfection sensitivity, Aerospace Science and Technology 62 (Supplement C) (2017) 114 – 121. doi:https://doi.org/10.1016/j.ast.2016.12.002.

[4] S. B. Biggers, S. Srinivasan, Compression buckling response of tailored rectangular composite plates, AIAA Journal 31 (3) (1993) 590–596. doi:https://doi.org/10.2514/3.61543.

[5] S. Nagendra, D. Jestin, Z. Gürdal, R. Haftka, L. Watson, Improved genetic algorithm for the design of stiffened composite panels, Computers & Structures 58 (3) (1996) 543 – 555. doi:https://doi.org/10.1016/0045-7949(95)00160-I.

[6] Z. Wu, P. M. Weaver, G. Raju, B. C. Kim, Buckling analysis and optimisation of variable angle tow composite plates, Thin-Walled Structures 60 (Supplement C) (2012) 163 – 172. doi:https://doi.org/10.1016/j.tws.2012.07.008.

[7] B. H. Coburn, P. M. Weaver, Buckling analysis, design and optimisation of variable-stiffness sandwich panels, International Journal of Solids and Structures 96 (Supplement C) (2016) 217 – 228. doi:https://doi.org/10.1016/j.ijsolstr.2016.06.007.

[8] E.Barkanov, O.Ozolins, E.Eglitis, F.Almeida, M.C.Bowering, G.Watson, Optimal design of composite lateral wing upper covers. Part I: Linear buckling analysis, Aerospace Science and Technology 38 (Supplement C) (2014) 1 – 8. doi:https://doi.org/10.1016/j.ast.2014.07.010.

[9] J. Thompson, Optimization as a generator of structural instability, International Journal of Mechanical Sciences 14 (9) (1972) 627–629.

[10] E. Barbero, A. Madeo, G. Zagari, R. Zinno, G. Zucco, Imperfection sensitivity analysis of laminated folded plates, Thin-Walled Structures 90 (2015) 128 – 139. doi:http://dx.doi.org/10.1016/j.tws.2015.01.017.

[11] E. Riks, An incremental approach to the solution of snapping and buckling problems, International Journal of Solids and Structures 15 (7) (1979) 529–551. doi:10.1016/0020-7683(79)90081-7.

[12] D. Magisano, L. Leonetti, G. Garcea, How to improve efficiency and robustness of the newton method in geometrically non-linear structural problem discretized via displacement-based finite elements, Computer Methods in Applied Mechanics and Engineering 313 (2017) 986–1005. doi:10.1016/j.cma.2016.10.023.

[13] Anders Eriksson and Costin Pacoste and Adam Zdunek, Numerical analysis of complex instability behaviour using incremental-iterative strategies, Computer Methods in Applied Mechanics and Engineering 179 (3) (1999) 265 – 305. doi:https://doi.org/10.1016/S0045-7825(99)00044-4.

[14] M. Deml and W. Wunderlich, Direct evaluation of the 'worst' imperfection shape in shell buckling, Computer Methods in Applied Mechanics and Engineering 149 (1) (1997) 201 – 222, containing papers presented at the Symposium on Advances in Computational Mechanics. doi:https://doi.org/10.1016/S0045-7825(97)00055-8.

[15] R.M.J. Groh and D. Avitabile and A. Pirrera, Generalised path-following for well-behaved nonlinear structures, Computer Methods in Applied Mechanics and Engineering 331 (2018) 394 – 426. doi:https://doi.org/10.1016/j.cma.2017.12.001.

[16] D. K. Shin, Z. Gurdal, O. H. Griffin, Jr., Minimum weight design of laminated composite plates for postbuckling performance, Applied Mechanics Reviews (1991) S219–S231doi:http://dx.doi.org/10.1115/1.3121359.

[17] E. Lindgaard, E. Lund, Nonlinear buckling optimization of composite structures, Computer Methods in Applied Mechanics and Engineering 199 (37) (2010) 2319 – 2330. doi:https://doi.org/10.1016/j.cma.2010.02.005.

[18] E. Lindgaard, E. Lund, K. Rasmussen, Nonlinear buckling optimization of composite structures considering "worst" shape imperfections, International Journal of Solids and Structures 47 (22) (2010) 3186 – 3202. doi:https://doi.org/10.1016/j.ijsolstr.2010.07.020.

[19] S. R. Henrichsen, E. Lindgaard, E. Lund, Robust buckling optimization of laminated composite structures using discrete material optimization considering "worst" shape imperfections, Thin-Walled Structures 94 (Supplement C) (2015) 624 – 635. doi:https://doi.org/10.1016/j.tws.2015.05.004.

[20] R. Degenhardt, A. Kling, K. Rohwer, A. Orifici, R. Thomson, Design and analysis of stiffened composite panels including post-buckling and collapse, Computers & Structures 86 (9) (2008) 919 – 929, composites. doi:https://doi.org/10.1016/j.compstruc.2007.04.022.

[21] Z. Wu, P. M. Weaver, G. Raju, Postbuckling optimisation of variable angle tow composite plates, Composite Structures 103 (Supplement C) (2013) 34 – 42. doi:https://doi.org/10.1016/j.compstruct.2013.03.004.

[22] D. Wang, M. M. Abdalla, W. Zhang, Buckling optimization design of curved stiffeners for grid-stiffened composite structures, Composite Structures 159 (Supplement C) (2017) 656 – 666. doi:https://doi.org/10.1016/j.compstruct.2016.10.013.

[23] W. Koiter, On the stability of elastic equilibrium, english transl. nasa tt-f10, 883 (1967) and affdl-tr70-25 (1970) Edition, Techische Hooge School at Delft, 1945.
[24] S. R. Henrichsen, P. M. Weaver, E. Lindgaard, E. Lund, Post-buckling optimization of composite structures using Koiter's method, International Journal for Numerical Methods in Engineering 108 (8) (2016) 902–940, nme.5239. doi:10.1002/nme.5239.
[25] D. Bushnell, Optimization of composite, stiffened, imperfect panels under combined loads for service in the postbuckling regime, Computer Methods in Applied Mechanics and Engineering 103 (1) (1993) 43 – 114. doi:https://doi.org/10.1016/0045-7825(93)90041-U.
[26] S. C. White, P. M. Weaver, Towards imperfection insensitive buckling response of shell structures-shells with plate-like post-buckled responses, The Aeronautical Journal 120 (1224) (2016) 233–253. doi:10.1017/aer.2015.14.
[27] R. L. Riche, R. T. Haftka, Optimization of laminate stacking sequence for buckling load maximization by genetic algorithm, AIAA Journal (1993). doi:doi: 10.2514/3.11710.
[28] K. Svanberg, The method of moving asymptotes—a new method for structural optimization, International Journal for Numerical Methods in Engineering 24 (2) (1987) 359–373. doi:10.1002/nme.1620240207.
URL http://dx.doi.org/10.1002/nme.1620240207
[29] L. S. Johansen, E. Lund, J. Kleist, Failure optimization of geometrically linear/nonlinear laminated composite structures using a two-step hierarchical model adaptivity, Computer Methods in Applied Mechanics and Engineering 198 (30) (2009) 2421 – 2438. doi:https://doi.org/10.1016/j.cma.2009.02.033.
[30] D. Magisano, L. Leonetti, G. Garcea, Koiter asymptotic analysis of multilayered composite structures using mixed solid-shell finite elements, Composite Structures 154 (2016) 296–308. doi:10.1016/j.compstruct.2016.07.046.
[31] G. Garcea, F. S. Liguori, L. Leonetti, D. Magisano, A. Madeo, Accurate and efficient a posteriori account of geometrical imperfections in Koiter finite element analysis, International Journal for Numerical Methods in Engineering 112 (9) (2017) 1154–1174, nme.5550. doi:10.1002/nme.5550.
[32] A. Madeo, R. Groh, G. Zucco, P. Weaver, G. Zagari, R. Zinno, Post-buckling analysis of variable-angle tow composite plates using Koiter's approach and the finite element method, Thin-Walled Structures 110 (2017) 1–13. doi:10.1016/j.tws.2016.10.012.
[33] D. Magisano, L. Leonetti, G. Garcea, Advantages of the mixed format in geometrically nonlinear analysis of beams and shells using solid finite elements, International Journal for Numerical Methods in Engineering 109 (9) (2017) 1237–1262. doi:10.1002/nme.5322.
[34] Z. B. Zabinsky, Random Search Algorithms, John Wiley & Sons, Inc., 2010. doi:10.1002/9780470400531.eorms0704.
URL http://dx.doi.org/10.1002/9780470400531.eorms0704
[35] K. Liang, M. Ruess, M. Abdalla, The koiter–newton approach using von kármán kinematics for buckling analyses of imperfection sensitive structures, Computer Methods in Applied Mechanics and Engineering 279 (2014) 440 – 468. doi:https://doi.org/10.1016/j.cma.2014.07.008.
URL http://www.sciencedirect.com/science/article/pii/S0045782514002308
[36] D. Magisano, K. Liang, G. Garcea, L. Leonetti, M. Ruess, An efficient mixed variational reduced-order model formulation for nonlinear analyses of elastic shells, International Journal for Numerical Methods in Engineering 113 (4) (2018) 634–655. doi:10.1002/nme.5629.
[37] R. Degenhardt, A. Kling, A. Bethge, J. Orf, L. Kärger, R. Zimmermann, K. Rohwer, A. Calvi, Investigations on imperfection sensitivity and deduction of improved knock-down factors for unstiffened cfrp cylindrical shells, Composite Structures 92 (8) (2010) 1939 – 1946. doi:https://doi.org/10.1016/j.compstruct.2009.12.014.
[38] G. Garcea, A. Madeo, G. Zagari, R. Casciaro, Asymptotic post-buckling FEM analysis using corotational formulation, International Journal of Solids and Structures 46 (2) (2009) 377–397.
[39] K. Sze, W. Chan, T. Pian, An eight-node hybrid-stress solid-shell element for geometric non-linear analysis of elastic shells, International Journal for Numerical Methods in Engineering 55 (7) (2002) 853–878. doi:10.1002/nme.535.
[40] L. Leonetti, F. Liguori, D. Magisano, G. Garcea, An efficient isogeometric solid-shell formulation for geometrically nonlinear analysis of elastic shells, Computer Methods in Applied Mechanics and Engineering 331 (2018) 159–183. doi:10.1016/j.cma.2017.11.025.
[41] R. Casciaro, G. Garcea, G. Attanasio, F. Giordano, Perturbation approach to elastic post-buckling analysis, Computers & Structures 66 (5) (1998) 585–595.
[42] G. Garcea, A. Madeo, R. Casciaro, Nonlinear FEM analysis for beams and plate assemblages based on the implicit corotational method, J. Mech. Mater. Struct. 7 (6) (2012) 539–574. doi:10.2140/jomms.2012.7.539.
[43] G. Zagari, G. Zucco, A. Madeo, V. Ungureanu, R. Zinno, D. Dubina, Evaluation of the erosion of critical buckling load of cold-formed steel members in compression based on Koiter asymptotic analysis, Thin-Walled Structures 108 (2016) 193–204. doi:10.1016/j.tws.2016.08.011.